Doctoral Dissertation

Meson-Meson Interactions in the One-Meson-Exchange Model

NGO THI HONG XIEM

GIFU UNIVERSITY

Yanagido 1-1, Gifu, Japan
2016

Doctoral Dissertation

Meson-Meson Interactions in the One-Meson-Exchange Model

By

NGO THI HONG XIEM

SUBMITTED IN PARTIAL FULFILLMENT OF THE
REQUIREMENTS FOR THE DEGREE OF
DOCTOR OF PHYLOSOPHY IN ENGINEERING

AT
GIFU UNIVERSITY
GIFU, JAPAN

August 2016

Abstract

In this dissertation, the meson-meson interactions at low-energies ($\sqrt{s} < 1.5$ GeV) with strangeness $S = 0, 1, 2$ are investigated in the $SU(3)$-symmetric one-meson-exchange model. In the model, both s- and t-channel exchange diagrams are considered in $\pi\pi - K\bar{K} - \pi\eta - \eta\eta$ and $\pi K - \eta K$ scatterings, in which, the coupling constants and cut-off masses in form factors are determined to reproduce experimental phase shifts with $J < 3$. The form factors are examined both in monopole and Gaussian types. At the same time, properties of KK interaction with $J = 0 \sim 3$ are predicted and we find an attractive KK interaction in the isospin $I = 0$, P-wave. By comparing the model which include η meson and the one without η meson, the effects of η channel in $\pi\pi$ and πK scatterings are discussed and we clarify important roles of η meson in the meson-meson interaction. Related to the resonances in meson-meson scatterings, we find the resonance poles corresponding to $a_0(980)$, $f_0(980)$, $f_2(1270)$, $\kappa(1430)$, $\kappa(700)$, $\rho(770)$, $K^*(982)$, $\phi(1020)$, $\sigma_1(400)$ and $\sigma_2(600)$. Their masses and widths are determined by pole positions of the S-matrix calculated on the complex E-plane. The existence of two poles σ_1 and σ_2 in the isospin $I = 0$, S-wave of the $\pi\pi - K\bar{K} - \eta\eta$ coupling is one of the very interesting point in this dissertation. In addition, to be one of the excited future plan, we discuss in brief about the compositeness of two-body resonance.

This page is intentionally left blank.

Acknowledgements

There are many people without whom this work would not have been possible.

Firstly, I would like to express my sincere gratitude to my advisor Professor Shoji Shinmura for the support of my Ph.D study and related research, for his patience, encouragement, and immense knowledge. His guidance helped me in all the time of research and writing of this dissertation. I could not have imagined having a better advisor and mentor for my Ph.D study.

My great thanks are due to Vietnamese and Japanese friends for their kind help and concern in many ways.

Finally, my warmest and most grateful thanks are due to my family, especially to my younger brother, Ngo Quang Thin, who gave me a place to live and work when I am in Gifu. I would like to express my deep thanks to my parents, who made every effort to provide me with the excellent basic education, on which all of my progress is based. Last but not least, I would like to thank my husband Nguyen Tien Dong for his technical support, understanding and love during the past few years. His support and encouragement make me strong to continue the Ph.D life. And thank you for my son, Nguyen Tien Nguyen Khoi, who help me realize the meaning of motherhood and how strong a mother can be.

Ngo Thi Hong Xiem

Gifu, Japan
August 28, 2016

This page is intentionally left blank.

Contents

Chapter 1

Introduction

The theoretical model of meson-meson interactions is one of the fundamental subjects in hadron physics. In view of the strong interaction, the physical mechanism of meson-meson interactions is thought to be similar to that of baryon-baryon interactions. But, because the masses of pseudoscalar mesons, π, K and η are smaller than baryons, relativistic effects in their interactions are expected to be essential. Therefore, it is not easy to investigate quantitatively their interactions.

There are three typical theoretical approaches to understand the interactions between two hadrons, that is, the lattice QCD (LQCD), the chiral perturbation models and hadron-exchange models. Each of these approaches plays a complementary role in understanding the hadron-hadron interactions.

The LQCD approach is a direct application of the fundamental theory of the strong interaction QCD to hadronic interactions and is expected to give model-independent reliable results [1–3]. At present, however, this approach cannot treat the meson-meson interactions at low energies. This approach is a kind of computer simulations and cannot make physical mechanisms in hadronic interactions clear.

In the second approach, the $SU(3)$ and $SU(2)$ chiral perturbation models have been treated for two decades. J. A. Oller and E. Oset [4] have used a non-perturbative coupled-channel approach to deal with the meson-meson interactions in the strangeness $S = 0$ sector at energies below $\sqrt{s} = 1.2$ GeV and the similar approach to $S = 0$ and $S = 1$ sectors have been attempted by J. A. Oller, E. Oset and J. R. Pelaez [5]. These approaches give understanding of low-energy hadronic interactions based on the fundamental symmetry. But, in general, these calculations are much changed in the higher-order calculations. Therefore, in this approach, it is difficult to clarify the effective degrees of freedom in the low-energy interactions.

In the third approach, the hadron-exchange models for baryon-baryon and meson-baryon interactions are extended to the meson-meson interactions. As explained in the next chapter, this approach has a long history and has been established as a model of low-energy baryon-baryon interactions. In this dissertation, we employ this approach and

clarify its applicability to the meson-meson interactions.

At low energies, the coupled-channel hadron-hadron interactions are classified into three kinds of interaction, that is, the baryon-baryon, the meson-baryon and the meson-meson interactions. This work, the investigation of meson-meson interaction, is one of the tasks to construct a unified hadron-hadron potential model which appropriate for all baryon-baryon [6], meson-baryon [7] and meson-meson interactions.

As given in Appendix A, we have many coupled-channel problems. In this dissertation, we pick up only the meson-meson sector, that is,

$S=-2$	$\bar{K}\bar{K}$
$S=-1$	$\pi\bar{K}-\eta\bar{K}$
$S=0$	$\pi\pi-K\bar{K}-\eta\pi-\eta\eta$
$S=1$	$\pi K-\eta K$
$S=2$	KK

In this dissertation, we not only construct the $\pi\pi-K\bar{K}-\pi\eta-\eta\eta$ and $\pi K-\eta K$ interactions but also give the quantitative results for the phase shifts of the $KK(\bar{K}\bar{K})$ scattering based on the $SU(3)$-symmetric one-meson-exchange interactions. Concretely, by using the common parameters (coupling constants and form factors), we determine the coupled-channel $\pi\pi-K\bar{K}-\pi\eta-\eta\eta$ and $\pi K-\eta K$ potentials in order to reproduce low-energy ($\sqrt{s}<1.5$ GeV) phase shifts of the isospin $I=0,1,\frac{1}{2}$, S- and P-wave $\pi\pi$ and πK scattering and predictive quantitative phase shifts of the KK scattering. Moreover, we also determine the physical masses and widths of $a_0(980)$, $f_0(980)$, $f_2(1270)$, $\kappa(1430)$, $\kappa(700)$, $\rho(770)$, $K^*(982)$, $\phi(1020)$, $\sigma_1(400)$ and $\sigma_2(600)$ through the S-matrix calculations on the complex-E plane. The existence of the two σ poles in the isospin $I=0$, S-wave of the coupled-channel $\pi\pi-K\bar{K}-\pi\eta-\eta\eta$ scattering also is one of the interesting discussion in this dissertation. In addition, by comparing the model which includes η meson and the one which does not contain η meson, we understand the important and necessary roles of the η meson in the short-range part of the meson-meson interaction. The brief investigation of the field renormalization to understand the quantitative measure of compositeness of the two-body resonances will be very interesting discussion point in this dissertation.

Because of the charge conjugation invariance of the strong interaction, we treat only $S=0,1,2$ sectors.

After the introduction, this dissertation are classified into five chapters. In chapter 2, we give a brief introduction about the one-meson-exchange model. The vector, scalar and tensor meson-exchange potentials are determined based on the $SU(3)$-symmetric interaction Lagrangians. The method, which is used to calculate the potentials, is described in details in section 2.4. The potentials are given in the momentum space. In chapter 3,

we explain the formalism of coupled-channel two-body problem for meson-meson scattering. The coupled-channel Lippmann-Schwinger (LS) equations are solved with relativistic kinematics in order to obtain the T-matrix. The S-matrix is then acquired from the on-shell T-matrix. Solutions of the LS equations are obtained by a kind of numerical matrix inversion methods which was developed by Haftel and Tabakin [8]. In s-channel exchange diagrams, we introduce bare masses for exchanged mesons and perform renormalization calculations to determine the poles of the S-matrix which correspond to physical resonance poles. In order to discuss the η-channel effects, we consider the potential model without η-channels. We find that the η-channel effects are not small but these effects can be fairly well compensated by the readjustment of coupling constants and form factors mainly in s-channel exchange diagrams.

In chapter 4, the numerical results of phase shifts calculated with our meson-meson interactions are shown compared with experimental analysis as well as quantitative predictions for KK interaction are given. Chapter 5 is devoted discussion about the effects of η channels in $\pi\pi - K\bar{K} - \pi\eta - \eta\eta$ and $\pi K - \eta K$ scatterings. The last chapter (chapter 6) gives the conclusion of this dissertation and proposes some future plans to refine our model.

This page is intentionally left blank.

Chapter 2

One-meson-exchange (OME) model

In this chapter, we describe briefly the history of the one-meson-exchange model of hadron-hadron interactions and how we apply this model in the meson-meson interactions.

2.1 History of OME model

One-meson exchange (OME) term means that we use one meson as a transfer particle to make the interactions between the two other particles. We can divide the nuclear force into three regions as in Fig. 2.1 [9]. The long-range part of the nuclear force is established by the one-pion exchange (OPE). In the intermediate-range part, the two-pion exchange (TPE) is supposed to dominate. In the short-range part, there are many different processes such as multi-pion, heavy-meson and quark-gluon exchange. However, a serious problem, that is, it is impossible to derive a sufficient spin-orbit force to explain the experimental NN scattering, occurred when the TPE contributes to the NN interaction. For this reason, the one-boson exchange (OBE) model was suggested to look for heavy vector bosons in order to explain the well-established, short-range spin-orbit force. Extending the framework of the previous work, the investigation of the short-range and the first-half of intermediate-range regions of the meson-meson interaction is described by the one-meson exchange (OME).

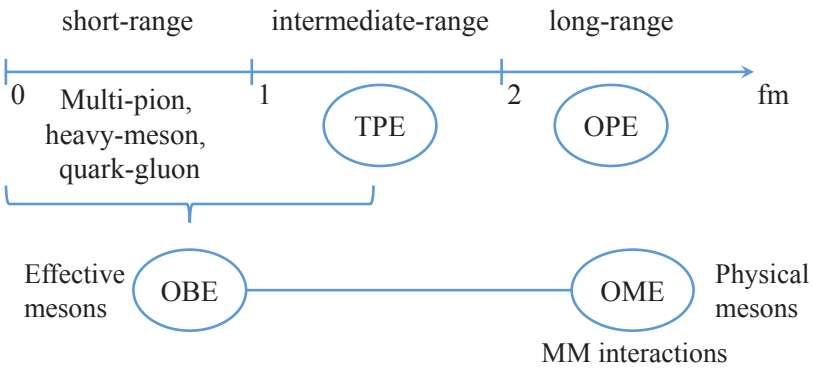

Figure 2.1: *Three regions of the nuclear force.*

2.2 OME diagrams

To understand how the interactions happen, we model them as the exchange diagrams. Normally, the exchange diagrams are divided into three types: s-, t-, and u-channel exchange diagrams. Our model has the t- and s-channel exchange diagrams (see Fig. 2.2). It is not necessary to treat the u-channel exchange, because it is already taken into account as the t-channel exchange. For example, the K^* exchange in πK interaction, which provides an exchange force, is regarded as a t-channel exchange ($t = (p'_{K^*} - p_\pi)^2$).

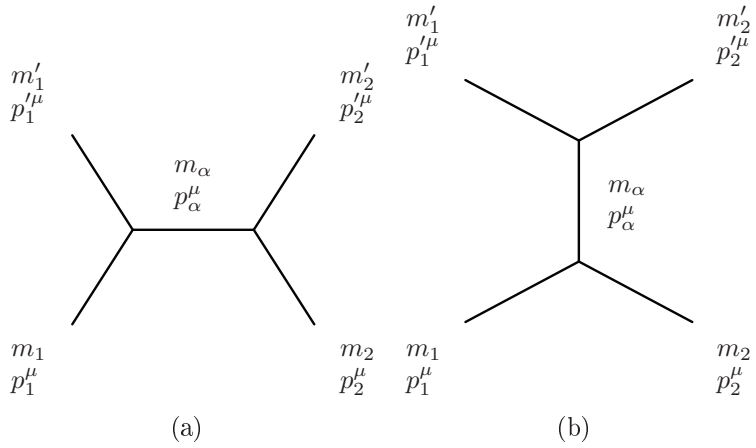

Figure 2.2: *Feynman diagrams. (a) t-channel (b) s-channel.*

We use $\rho, K^*, \omega, \phi, f_2, \epsilon, \kappa, a_0$ as exchanged mesons. We emphasize that K^*, both t- and s-channels exchange diagrams have to be taken into account in the $\pi\pi$ and πK interactions to get a quantitative description of the experimental phase shifts. The scalar-isoscalar $\epsilon(1400)$, the isoscalar tensor (spin-two) meson $f_2(1270)$, and the strange scalar meson $\kappa(1430)$ in s-channel exchange are necessary but their t-channel contributions are neglected because their large masses bring too short-range interaction. KK interaction acts only on t-channel exchange diagrams with ρ, ω and ϕ meson-exchange. When extending the model for investigating the effect of $\eta\eta$ and $\eta\pi$ channels in $\pi\pi$ scattering and ηK in πK scattering, we consider the ϵ and K^*-exchange contributions.

As listed in Tables 2.1 - 2.6, we consider many exchange diagrams in the strangeness $S = 0, 1$ and 2 sectors. The numbers in the column 5 are the isospin factors. The term LF which used in the column 6 of all the tables are the momentum factors.

2.3 The interaction Lagrangians and coupling constants

For scalar-meson exchange, we have two possible interaction Lagrangians,

$$\mathcal{L}_{pps} = g_{pps} m_p \phi_p(x) \phi_p(x) \phi_s(x) \qquad \text{(scalar coupling)} \tag{2.1}$$

or

$$\mathcal{L}_{pps} = \frac{f_{pps}}{m_p} \partial^\mu \phi_p(x) \partial_\mu \phi_p(x) \phi_s(x) \qquad \text{(derivative coupling).} \tag{2.2}$$

Table 2.1: *s-channel vector-meson exchange diagrams* ($S = 0$)

initial mesons	final mesons	exchanged meson	Isospin	factor	LF
$\pi\pi$	$\pi\pi$	ρ	1	8	-1
πK	πK	K^*	$\frac{1}{2}$	-3	-1
$\bar{K}K$	$\bar{K}K$	ρ	1	-2	-1
$\bar{K}K$	$\bar{K}K$	ϕ	0	-2	-1
$\bar{K}K$	$\bar{K}K$	ω	0	-1	-1
$\pi\pi$	$\bar{K}K$	ρ	1	4	-1

Table 2.2: *t-channel vector-meson exchange diagrams* ($S = 0, 1$)

initial mesons	final mesons	exchanged meson	Isospin	factor	LF
$\pi\pi$	$\pi\pi$	ρ	2	4	1
$\pi\pi$	$\pi\pi$	ρ	1	-4	1
$\pi\pi$	$\pi\pi$	ρ	0	-8	1
$\pi\pi$	$\bar{K}K$	K^*	1	2	1
$\pi\pi$	$\bar{K}K$	K^*	0	$\sqrt{6}$	1
$\bar{K}K$	$\bar{K}K$	ρ	1	1	1
$\bar{K}K$	$\bar{K}K$	ρ	0	-3	1
$\bar{K}K$	$\bar{K}K$	ϕ	1	-2	1
$\bar{K}K$	$\bar{K}K$	ϕ	0	-2	1
$\bar{K}K$	$\bar{K}K$	ω	1	-1	1
$\bar{K}K$	$\bar{K}K$	ω	0	-1	1
πK	πK	ρ	$\frac{3}{2}$	2	1
πK	πK	ρ	$\frac{1}{2}$	-4	1
πK	πK	K^*	$\frac{3}{2}$	2	$(-1)^J$
πK	πK	K^*	$\frac{1}{2}$	-1	$(-1)^J$
πK	πK	K^*	$\frac{3}{2}$	-2	$(-1)^J$
πK	πK	K^*	$\frac{1}{2}$	1	$(-1)^J$

Table 2.3: *t-channel vector-meson exchange diagrams* ($S = 0, 1$)

initial mesons	final mesons	exchanged meson	Isospin	factor	LF
πK	ηK	K^*	$\frac{1}{2}$	-2.74232	$(-1)^J$
$\bar{K}K$	$\pi\eta$	K^*	1	2.23909	1
$\bar{K}K$	$\eta\eta$	K^*	0	-3.54510	1
ηK	ηK	K^*	$\frac{1}{2}$	2.50677	$(-1)^J$

Table 2.4: *s-channel vector-meson exchange diagrams* ($S = 1$)

initial mesons	final mesons	exchanged meson	Isospin	factor	LF
πK	ηK	K^*	$\frac{1}{2}$	2.74232	-1
ηK	ηK	K^*	$\frac{1}{2}$	-2.50677	-1

Table 2.5: *t-channel vector-meson exchange diagrams* ($S = 2$)

initial mesons	final mesons	exchanged meson	Isospin	factor	LF
KK	KK	ρ	1	1	1
KK	KK	ρ	0	-3	1
KK	KK	ϕ	1	2	1
KK	KK	ϕ	0	2	1
KK	KK	ω	1	1	1
KK	KK	ω	0	1	1

Table 2.6: *s-channel scalar- and tensor-meson exchange diagrams* ($S = 0, 1$)

initial mesons	final mesons	exchanged meson	Isospin	factor	LF
$\pi\pi$	$\pi\pi$	f_2	0	3	1
$\pi\pi$	$\bar{K}K$	f_2	0	3	1
$\pi\pi$	$\eta\eta$	f_2	0	3	1
$\bar{K}K$	$\bar{K}K$	f_2	0	3	1
$\bar{K}K$	$\eta\eta$	f_2	0	3	1
$\eta\eta$	$\eta\eta$	f_2	0	3	1
πK	πK	κ	$\frac{1}{2}$	2	1
πK	ηK	κ	$\frac{1}{2}$	2	1
ηK	ηK	κ	$\frac{1}{2}$	2	1
$\bar{K}K$	$\bar{K}K$	a_0	1	1	1
$\pi\eta$	$\bar{K}K$	a_0	1	1	1
$\pi\eta$	$\pi\eta$	a_0	1	1	1
$\pi\pi$	$\pi\pi$	ε_1	0	2	1
$\bar{K}K$	$\bar{K}K$	ε_1	0	2	1
$\bar{K}K$	$\pi\pi$	ε_1	0	2	1
$\eta\eta$	$\pi\pi$	ε_1	0	2	1
$\eta\eta$	$\bar{K}K$	ε_1	0	2	1
$\eta\eta$	$\eta\eta$	ε_1	0	2	1

In this work, we employ the latter type of coupling (derivative coupling) because this type seems to be preferable by the low energy theorem.

For vector- and tensor-meson exchange, we assume

$$\mathcal{L}_{ppv} = g_{ppv}\phi_p(x)\partial_\mu\phi_p(x)\phi_s^\mu(x) \tag{2.3}$$

and

$$\mathcal{L}_{ppt} = g_{ppt}\frac{2}{m_\pi}\partial^\mu\phi_p(x)\partial_\nu\phi_p(x)\phi_t^{\mu\nu} \tag{2.4}$$

respectively, which are commonly used in theoretical models. Where $\phi_s, \phi_p, \phi_\nu^\mu$, and $\phi_t^{\mu\nu}$ are the field operators for scalar, pseudoscalar, vector, and tensor mesons, respectively.

For meson-meson-meson vertices, we explain the $SU(3)$-symmetric coupling constants. For scalar, vector and tensor mesons, the $SU(3)$-symmetric Lagrangians are given by:

$$\begin{aligned}
\mathcal{L}_{pps} &= \frac{F_s}{m_\pi}\mathrm{Tr}[(\partial^\mu P\partial_\mu P)S], \\
\mathcal{L}_{ppv} &= G_v\mathrm{Tr}[(\partial^\mu P)P - P(\partial^\mu P)V], \\
\mathcal{L}_{ppt} &= F_t\frac{2}{m_\pi}\mathrm{Tr}[(\partial_\mu P)(\partial^\nu P)T^{\mu\nu}],
\end{aligned} \tag{2.5}$$

respectively. P is the 3×3 matrix representation of the pseudoscalar octet, $P=\lambda^a P^a$, $a=1,...,8$ and λ^a are the 3×3 generators of $SU(3)$.

$$P_8=\begin{pmatrix} \frac{\pi^0}{\sqrt{2}}+\frac{\eta_8}{\sqrt{6}} & \pi^+ & K^+ \\ \pi^- & -\frac{\pi^0}{\sqrt{2}}+\frac{\eta_8}{\sqrt{6}} & K^0 \\ K^- & \bar{K^0} & -\sqrt{\frac{2}{3}}\eta_8 \end{pmatrix}, \qquad P_1=\eta_1, \tag{2.6}$$

$$V_8=\begin{pmatrix} \frac{\rho^0}{\sqrt{2}}+\frac{\phi}{\sqrt{6}} & \rho^+ & K^{*+} \\ \rho^- & -\frac{\rho^0}{\sqrt{2}}+\frac{\phi}{\sqrt{6}} & K^{*0} \\ K^{*-} & \bar{K}^{*0} & -\sqrt{\frac{2}{3}}\phi \end{pmatrix}, \qquad V_1=\omega, \tag{2.7}$$

$$S_8=\begin{pmatrix} \frac{a_0}{\sqrt{2}}+\frac{f_0}{\sqrt{6}} & a^+ & \kappa^+ \\ a^- & -\frac{a_0}{\sqrt{2}}+\frac{f_0}{\sqrt{6}} & \kappa^0 \\ \kappa^- & \bar{\kappa}^0 & -\sqrt{\frac{2}{3}}f_0 \end{pmatrix}, \qquad S_1=\epsilon. \tag{2.8}$$

For tensor meson f_2 and scalar meson ϵ_1, we assume them to be the flavor $SU(3)$ singlet mesons ($T_1=f_2$ and $S_1=\epsilon$). In above expressions, we assume symmetric (D-type) coupling for scalar and tensor mesons and anti-symmetric (F-type) one for vector mesons. The singlet-octet mixing angles θ_V and θ_P for vector and pseudoscalar mesons are introduced by:

$$\begin{aligned} \omega^{phys} &= \omega\cos\theta_V+\phi\sin\theta_V, & \phi^{phys} &= \phi\cos\theta_V-\omega\sin\theta_V, \\ \eta_1^{phys} &= \eta_1\cos\theta_P+\eta_8\sin\theta_P, & \eta_8^{phys} &= \eta_8\cos\theta_P-\eta_1\sin\theta_P. \end{aligned} \tag{2.9}$$

The values θ_P, θ_V are determined based on the quark models, $\theta_P=24^o$ by the Gell-Mann-Okubo mass formula, $\theta_V=35.3^o$ by the ideal mixing between ω and ϕ. By using the $SU(3)$ coupling constants and the mixing angles θ_P, θ_V, we determined the coupling constants g_{abc}, which correspond to g_1 and g_2 in the Eqs. (2.13), (2.15) and (2.17).

2.4 Coupled-channel meson-meson potentials in the OME model

In our calculations, all kinematical variables are defined in the center of mass system of interacting two mesons and employ relativistic kinematics. In practice, using the notation as Fig. 2.2, we define:

$$p_1^\mu=(\omega_1,\mathbb{p}_1), \qquad p_1^{'\mu}=(\omega_1^{'},\mathbb{p}_1^{'}), \qquad p_\alpha^\mu=(\omega_\alpha,\mathbb{p}_\alpha),$$

$$p_2^{'\mu} = (\omega_2^{'}, \mathbb{p}_2^{'}), \qquad \mathbb{p}_2^{'} = -\mathbb{p}_1^{'}, \qquad p_2^{\mu} = (\omega_2, \mathbb{p}_2), \qquad \mathbb{p}_2 = -\mathbb{p}_1, \qquad \mathbb{q}_\alpha = \mathbb{p}_1 - \mathbb{p}^{'}{}_1,$$

$$\begin{aligned} \omega_1 &= \sqrt{{m_1}^2 + {\mathbb{p}_1}^2}, & \omega_1' &= \sqrt{{m_1'}^2 + {\mathbb{p}_1'}^2}, \\ \omega_2 &= \sqrt{{m_2}^2 + (-\mathbb{p}_1)^2}, & \omega_2' &= \sqrt{{m_2'}^2 + (-\mathbb{p}_1')^2}, \end{aligned} \tag{2.10}$$

$$\omega_\alpha = \sqrt{m_\alpha^2 + \mathbb{q}_\alpha^2} = \sqrt{m_\alpha^2 + {p_1'}^2 + {p_1}^2 - 2p_1' p_1 \cos\theta}.$$

The above equations are applied for t-channel exchange. And for s-channel exchange, almost equations are the same but:

$$\mathbb{q}_\alpha = 0, \qquad\qquad \omega_\alpha = m_\alpha. \tag{2.11}$$

For vector-exchange, by using the property of the massive vector particle, we always find,

$$\sum_{\lambda_\alpha} \epsilon^\mu(\mathbb{p}_\alpha, \lambda_\alpha)\epsilon^{*\nu}(\mathbb{p}_\alpha, \lambda_\alpha) = -g^{\mu\nu} + \frac{p_\alpha^\mu p_\alpha^\nu}{m_\alpha^2}. \tag{2.12}$$

where, $\epsilon^\mu(\mathbb{p}_\alpha, \lambda_\alpha)$ is the polarization vector for vector meson with momentum $\mathbb{p}_\alpha$ and helicity λ_α. By using the interaction Lagrangian $\mathcal{L}_{ppv}$ given in Eq. (2.3), we obtained the potential for t-channel vector meson-exchange given by:

$$\begin{aligned} \langle 1'2'|V_v^{(t)}(z)|12\rangle = {} & \frac{g_1 g_2}{(2\pi)^3} F_1^{(t)}(\mathbb{q}_\alpha^2) F_2^{(t)}(\mathbb{q}_\alpha^2) \frac{1}{8\omega_\alpha \sqrt{\omega_1'\omega_2'\omega_1\omega_2}} (p_1^{'} + p_1)_\mu (p_2^{'} + p_2)_\nu \\ & \times (-g^{\mu\nu} + \frac{p_\alpha^\mu p_\alpha^\nu}{m_\alpha^2}) \left(\frac{1}{z - \omega_1^{'} - \omega_2 - \omega_\alpha} + \frac{1}{z - \omega_2^{'} - \omega_1 - \omega_\alpha} \right), \end{aligned} \tag{2.13}$$

where z is a variable corresponding to total energy $\sqrt{s}$. The form factors $F^{(t)}$ will be given in section 2.5. We need an additional factor $\sqrt{\frac{1}{2}}^k$ with $k = 0$ when both of initial and final states consist of different particles, $k = 1$ when one of states consist of identical particles, $k = 2$ for both identical.

For the potential by s-channel vector-meson-exchange, we obtain:

$$\begin{aligned} \langle 1'2'|V_v^{(s)}(z)|12\rangle = {} & \frac{g_1 g_2}{(2\pi)^3} F_1^{(s,1)}(\omega_p^2) F_2^{(s,1)}(\omega_p'^2) \frac{1}{8 m_\alpha \sqrt{\omega_1'\omega_2'\omega_1\omega_2}} (p_1^{'} - p_1)_\mu p_2^{'} - p_2)_\nu \\ & \times (-g^{\mu\nu} + \frac{p_\alpha^\mu p_\alpha^\nu}{m_\alpha^2}) \left(\frac{1}{z - m_\alpha^0} + \frac{1}{z - \omega_1^{'} - \omega_2^{'} - \omega_1 - \omega_2 - m_\alpha} \right), \end{aligned} \tag{2.14}$$

where, $p_\alpha^\mu = (m_\alpha, 0)$, $\omega_p = \omega_1 + \omega_2$, $\omega_p' = \omega_1' + \omega_2'$ and m_α^0 is bare mass, m_α is physical mass.

The s-channel exchange potential for derivative coupling is given as following:

$$\langle 1'2'|V_s^{(s)}(z)|12\rangle = \frac{g_1 g_2}{(2\pi)^3} F_1^{(s,2)}(\omega_p^2) F_2^{(s,2)}(\omega_p'^2) \frac{1}{8m_\alpha \sqrt{\omega_1' \omega_2' \omega_1 \omega_2}} \times \left\{ \frac{1}{m_\pi^2} \left[(\omega_1' - \omega_2')^2 - 4P_1'^2 \right] \left[(\omega_1 - \omega_2)^2 - 4P_1^2 \right] \right\} \times \left(\frac{1}{z - m_\alpha^0} + \frac{1}{z - \omega_1' - \omega_2' - \omega_1 - \omega_1 - \omega_2 - m_\alpha} \right). \tag{2.15}$$

In order to calculate the potential by s-channel tensor meson (f_2 exchange), we need the polarization tensor of the spin-two meson:

$$\sum_{\lambda_\alpha} \epsilon^{\mu\nu}(\mathbb{p}_\alpha, \lambda_\alpha) \epsilon^{\rho\sigma}(\mathbb{p}_\alpha, \lambda_\alpha^*) = \frac{1}{2}(P^{\mu\rho}P^{\nu\sigma} + P^{\mu\sigma}P^{\nu\rho}) - \frac{1}{3}P^{\mu\nu}P^{\rho\sigma}, \tag{2.16}$$

where $P^{\mu\nu} = -g^{\mu\nu} + \dfrac{p_\alpha^\mu p_\alpha^\nu}{m_\alpha^2}$.

Then, the s-channel potential for tensor meson is given by:

$$\langle 1'2'|V_t^{(s)}(z)|12\rangle = \frac{g_1 g_2}{(2\pi)^3} F_1^{(s,2)}(\omega_p^2) F_2^{(s,2)}(\omega_p'^2) \frac{1}{8m_\alpha \sqrt{\omega_1' \omega_2' \omega_1 \omega_2}} \frac{2}{m_\pi} \times \frac{32}{3} \left(P_1' P_1\right)^2 P_2(\cos\theta) \left(\frac{1}{z - m_\alpha^0} + \frac{1}{z - \omega_1' - \omega_2' - \omega_1 - \omega_1 - \omega_2 - m_\alpha} \right), \tag{2.17}$$

where $P_2(\cos\theta)$ is the Legendre polynomial.

2.5 Form factors

Form factors play a very important role in meson-meson interactions. In this paper, we attempt two types of form factors: monopole [10] and Gaussian type [6, 7]. Meson-exchange potentials contain form factors which express the effects of short-range physics beyond one-meson exchange mechanism, for example, many-meson exchange or intrinsic structure of hadrons. Therefore, we treat the form factors as phenomenological quantities which are determined by fitting to the experimental data.

For t-channel exchange, the form factor of monopole type can be written as following:

$$F_m^{(t)}(\mathbb{q}_\alpha^2) = \frac{\Lambda^2 - m_\alpha^2}{\Lambda^2 + \mathbb{q}_\alpha^2}, \tag{2.18}$$

where m_α and $\mathbb{q}_\alpha$ are the mass and 3-momentum of the exchanged mesons in the t-channel exchange, respectively.

For s-channel exchange, we take two kinds of the monopole form factors:

$$F_m^{(s,1)}(\omega_p^2) = \frac{\Lambda^2 + m_\alpha^2}{\Lambda^2 + \omega_p^2}, \qquad \text{and} \qquad F_m^{(s,2)}(\omega_p^2) = \frac{\Lambda^4 + m_\alpha^4}{\Lambda^4 + \omega_p^4}, \tag{2.19}$$

where ω_p is the total energy of the incoming (outgoing) state. The forth order monopole type is necessary for the derivative coupling of the scalar meson as well as the tensor meson to obtain the sufficient convergence at the high momentum region.

The form factors of Gaussian type for t- and s-channel exchange are defined respectively by:

$$F_g^{(t)}(\mathbb{q}_\alpha^2) = e^{\frac{-\mathbb{q}_\alpha^2}{\Lambda^2}}, \tag{2.20}$$

$$F_g^{(s)}(\omega_p^2) = e^{-\frac{\omega_p^2}{\Lambda^2}}. \tag{2.21}$$

We should notice the difference between two kinds of form factors. In t-channel exchange, we have $F_m^{(t)}(\mathbb{q}_\alpha^2) < 1$ and $F_g^{(t)}(\mathbb{q}_\alpha^2) \sim 1$ for the momentum transfer $\mathbb{p}_\alpha \cong 0$, which corresponds to the forward scattering. In such situation, short-range physics does not work and the latter may be reasonable. On the other hand, in the s-channel exchange, $F_m^{(s,1)}(\omega_p^2) = F_m^{(s,2)}(\omega_p^2) = 1$ and $F_g^{(s)}(\omega_p^2) < 1$ for on-resonance scattering ($s = m_\alpha^2$). But, in this case, the "momentum transfer" $|\mathbb{p}_1| = |\mathbb{p}_2|$ is not small in general. Short-range properties of mesons may be responsible. Therefore, Gaussian form factors seem to be more reasonable than monopole ones.

This page is intentionally left blank.

Chapter 3

Coupled-channel formalism for meson-meson scattering

In this chapter, we introduce the coupled-channel formalisms for meson-meson scattering with two-body meson-meson interactions.

3.1 The Lippmann-Schwinger equation

It is convenient to use the reaction matrix R to explore further the structure of the momentum-space S-matrix. The operator R is defined by the relation $S = 1 + R$. Obviously R represents the difference between the actual value of S and its value in the absence of all interaction. We write the matrix element $\langle c'\mathbb{p}'|R|c\mathbb{p}\rangle$ as

$$\langle c'\mathbb{p}'|R|c\mathbb{p}\rangle = -2\pi i\delta(E^{c'}_{p'} - E^{c}_{p})t^{c'c}(\mathbb{p}' \leftarrow \mathbb{p}) \tag{3.1}$$

where c' and c are the labels of channels. For example, in $\pi\pi - \bar{K}K - \eta\pi - \eta\eta$ scattering, $c = 1(\pi\pi), = 2(\bar{K}K), = 3(\eta\pi), = 4(\eta\eta)$ are assigned.

The S-matrix is

$$\langle c'\mathbb{p}'|S|c\mathbb{p}\rangle = \delta_{c'c}\delta^3(\mathbb{p}' - \mathbb{p}) - 2\pi i\delta(E^{c'}_{p'} - E^{c}_{p})t^{c'c}(\mathbb{p}' \leftarrow \mathbb{p}) \tag{3.2}$$

It is not hard to understand the significance of the two terms in the decomposition of the S-matrix. The first term, $\delta_{c'c}\delta^3(\mathbb{p}' - \mathbb{p})$ is the amplitude for the particle to pass the force center without being scattered. The second term is the scattering amplitude from channel c to channel c'. We know that the particle is scattered when its momentum changes, while its energy stays the same. Thus, the second term in the Eq. (3.2) should conserve energy, but not the individual components of momentum. In the other word, the factor $t^{c'c}(\mathbb{p}' \leftarrow \mathbb{p})$ should be the smooth function of its arguments.

Since the Eq. (3.2) contain the factor $\delta(E^{c'}_{p'} - E^{c}_{p})$, the $t^{c'c}(\mathbb{p}' \leftarrow \mathbb{p})$ is only defined when $E^{c'}_{p'} - E^{c}_{p} = 0$. For this reason, $t^{c'c}(\mathbb{p}' \leftarrow \mathbb{p})$ is called the T-matrix on the energy shell, or simply is *on-shell T-matrix*. The matrix $\langle \mathbb{p}'|T|\mathbb{p}\rangle$ which is defined for all $\mathbb{p}'$ and $\mathbb{p}$, is called the *off-shell T-matrix*. The off-shell T-matrix is a useful tool in calculation, especially, it

satisfied the important Lippmann-Schwinger equation. The on-shell T-matrix is related to the scattering amplitude.

The Lippmann-Schwinger integral equation for $T^{c'c}(\mathbb{p}', \mathbb{p}, E) = \langle c'\mathbb{p}'|T(E)|c\mathbb{p}\rangle$ is written as

$$T^{c'c}(\mathbb{p}', \mathbb{p}, E) = V^{c'c}(\mathbb{p}', \mathbb{p}) + \sum_{c''} \int d^3\mathbb{p}'' V^{c'c''}(\mathbb{p}', \mathbb{p}'') \frac{1}{E - E^{c''}_{p''} + i\varepsilon} T^{c''c}(\mathbb{p}'', \mathbb{p}, E) \quad (3.3)$$

where $V^{c'c}(\mathbb{p}', \mathbb{p}) = \langle c'\mathbb{p}'|V|c\mathbb{p}\rangle$ is the matrix element of the two-body potential V. This equation is an integral type of the scattering problem. The LS equation is a fundamental result, as important as the Schrodinger equation for scattering theory. And both equations are proved to be equivalent physically. But in practical treatment, the former is convenient, especially in the case that the relativistic kinematics becomes important. In addition, the LS equation is easily extended to the Faddeev's equation of three-body problem through the off-shell T-matrix.

We introduce the partial wave expansion:

$$V^{c'c}_l(p'p|z) = 2\pi \int_{-1}^{1} d\cos\theta P_l(\cos\theta) \langle c'\mathbb{p}'|V(z)|c\mathbb{p}\rangle, \quad (3.4)$$

$$T^{c'c}_l(p'p|z) = 2\pi \int_{-1}^{1} d\cos\theta P_l(\cos\theta) \langle c'\mathbb{p}'|T(z)|c\mathbb{p}\rangle, \quad (3.5)$$

Using the LS equation given in (3.3), we obtain

$$T^{c'c}_l(p'p|z) = V^{c'c}_l(p'p|z) + \sum_{c''} \int dp'' p''^2 V^{c'c''}_l(p'p''|z) \frac{1}{z - E^{c''}_{p''} + i\varepsilon} T^{c''c}_l(p''p|z). \quad (3.6)$$

This equation is called the partial-wave Lippmann-Schwinger equation. To solve this equation, we must treat singularities at $z - E^c_p = 0$ for open channels c. To do so, we employ the method proposed by Halftel-Tabakin[8].

3.2 Phase shifts and cross sections

The asymptotic free motion of a particle after the collision is related to its initial state by the S-matrix. The most important properties of the S-matrix is that it conserves energy and momentum, and its matrix elements can be decomposed in terms of the scattering amplitude.

Taking the relativistic kinematics into consideration, we obtain the partial-wave S-matrix:

$$S^{c'c}_l(z) = \delta_{c'c} - 2\pi i \frac{\sqrt{p'_c p_c}}{\sqrt{s}} \sqrt{\omega^{c'}_1 \omega^{c'}_2 \omega^c_1 \omega^c_2} T^{c'c}_l(p'p|z) \quad (3.7)$$

where p_c, ω^c_1 and ω^c_2 are on-shell momentum and on-shell energies

$$\omega^c_1 = \sqrt{m^{c\,2}_1 + p^2_c}, \qquad \omega^c_2 = \sqrt{m^{c\,2}_2 + p^2_c},$$

for the channel c.

The phase shift δ_l^c is defined by

$$S_l^{cc}(z) = e^{2i\delta_l^c} \tag{3.8}$$

in case that only one channel c is open.

In the case of two open channels $c = 1, 2$, the S-matrix is parameterized by

$$S_l(z) = \begin{pmatrix} \eta_l(z)e^{2i\delta_l^1(z)} & i\sqrt{1-\eta_l^2(z)}e^{i[\delta_l^1(z)+\delta_l^2(z)]} \\ i\sqrt{1-\eta_l^2(z)}e^{i[\delta_l^1(z)+\delta_l^2(z)]} & \eta_l(z)e^{2i\delta_l^2(z)} \end{pmatrix} \tag{3.9}$$

where $\delta_l^1(z), \delta_l^2(z)$ are phase shifts in channels $c = 1, 2$, respectively, and $\eta_l(z)$ is so-called inelasticity parameter.

For the case with more than two open channels, we do not introduce phase shifts, but we use the S-matrix elements directly to describe scattering quantities.

In terms of the phase shifts δ_l, the cross section is given by

$$\sigma = \frac{4\pi}{k^2}\sum_l (2l+1)\sin^2\delta_l \tag{3.10}$$

It is interesting that there is a maximum possible value for the cross section for each partial wave. From Eq. (3.10), the cross section for a given partial wave l is

$$\sigma_l = \frac{4\pi}{k^2}(2l+1)\sin^2\delta_l \leq \frac{4\pi}{k^2}(2l+1). \tag{3.11}$$

The maximum is obtained for the phases shift $\delta_l = \pm\pi/2$. This is called unitarity limit, as it is a consequence of the unitarity of the S-matrix.

3.3 The method to treat a singularity in $V_l^{c'c}(p'p|z)$

We start with the partial wave expansion of the potential $V_l^{c'c}(p'p|z)$.

$$V_l^{c'c}(p'p|z) = 2\pi\int_{-1}^{1} d\cos\theta P_l(\cos\theta)\langle c'\mathbb{p}'|V(z)|c\mathbb{p}\rangle \tag{3.12}$$

where θ is the angle between $\mathbb{p}$ and $\mathbb{p}'$.

We need carefully treatment of above integration due to a singularity. To treat the singularity, we use the method developed by Buttgen et al.[11]. We explain this method in the case of the t-channel exchange potential. We define

$$\begin{aligned} f(p', p, \cos\theta) \equiv\ & 2\pi\frac{g_1 g_2}{(2\pi)^3}F^{(t)^2}(\mathbb{q}_\alpha^2)\frac{1}{8\omega_\alpha(\omega_1'\omega_2'\omega_1\omega_2)^{1/2}} \\ & \times\Big\{-\Big[(\omega_1'+\omega_1)(\omega_2'+\omega_2)+p'^2+p^2+2p'p\cos\theta\Big] \\ & +\Big[(\omega_1'+\omega_1)\omega_\alpha - p^2 + p'^2\Big]\Big[(\omega_2'+\omega_2)\omega_\alpha + p^2 - p'^2\Big]\frac{1}{m_\alpha^2}\Big\}P_l(\cos\theta) \end{aligned} \tag{3.13}$$

and the potential can be rewritten as

$$V_l^{c'c}(p'p|z) = \int_{-1}^{1} d\cos\theta \frac{f(p',p,\cos\theta)}{\omega_\alpha(z-\omega_1'-\omega_2-\omega_\alpha+i\varepsilon)} + \int_{-1}^{1} d\cos\theta \frac{f(p',p,\cos\theta)}{\omega_\alpha(z-\omega_2'-\omega_1-\omega_\alpha+i\varepsilon)} \tag{3.14}$$

We consider a general form

$$I(p'p|z) = \int_{-1}^{1} d\cos\theta \frac{f(p',p,\cos\theta)}{\omega_\alpha(z-E-\omega_\alpha+i\varepsilon)} \tag{3.15}$$

where $E = \omega_1' + \omega_2$ and $E = \omega_2' + \omega_1$ correspond to the first term and the second term, respectively. ω_α is defined by

$$\omega_\alpha = \sqrt{m_{ex}^2 + p'^2 + p^2 - 2p'p\cos\theta}. \tag{3.16}$$

If the condition

$$\sqrt{m_{ex}^2 + p'^2 + p^2 + 2p'p} \geq z - E \geq \sqrt{m_{ex}^2 + p'^2 + p^2 - 2p'p} \quad (>0) \tag{3.17}$$

is satisfied, we find a singularity at

$$\cos\theta = \frac{(z-E)^2 - m_{ex}^2 - p'^2 - p^2}{2p'p}. \tag{3.18}$$

In such case

$$I(p'p|z) = \mathcal{P}\int_{-1}^{1} d\cos\theta \frac{f(p',p,\cos\theta)}{\omega_\alpha(z-E-\omega_\alpha)} - i\pi\int_{-1}^{1} d\cos\theta \frac{f(p',p,\cos\theta)}{\omega_\alpha}\delta(z-E-\omega_\alpha). \tag{3.19}$$

Let $\xi = \cos\theta$, we have

$$I(p'p|z) = \mathcal{P}\int_{-1}^{1} d\xi \frac{f(p',p,\xi)}{\omega_\alpha(z-E-\omega_\alpha)} - i\pi\int_{-1}^{1} d\xi \frac{f(p',p,\xi)}{\omega_\alpha}\delta(z-E-\omega_\alpha) \tag{3.20}$$

with

$$\omega_\alpha = \sqrt{m_{ex}^2 + p'^2 + p^2 - 2p'p\xi}. \tag{3.21}$$

By using

$$\delta\left(g(\xi)\right) = \frac{1}{|g'(\xi_0)|}\delta(\xi-\xi_0) \tag{3.22}$$

where

$$g(\xi_0) = 0, \tag{3.23}$$

$$g(\xi) = z - E - \omega_\alpha, \tag{3.24}$$

$$g'(\xi_0) = \frac{p'p}{\omega_\alpha(\xi_0)}, \tag{3.25}$$

finally, we obtain

$$I(p'p|z) = \int_{-1}^{1} d\xi \left[\frac{f(p',p,\xi)}{\omega_\alpha(z-E-\omega_\alpha)} - \frac{f(p',p,\xi_0)}{p'p}\frac{1}{\xi-\xi_0}\right] + \frac{f(p',p,\xi_0)}{p'p}\left\{\ln\left|\frac{1-\xi_0}{1+\xi_0}\right| - i\pi\right\} \tag{3.26}$$

In above expression, the singularity at $\xi = \xi_0$ disappears from the integrand.

3.4 The renormalization with the s-channel-exchange potentials

For s-channel-exchange potentials, we introduced the bare mass m_α^0 and (bare) coupling constants g_1, g_2 in Eq. (2.13), (2.14), (2.15) and (2.17). As a result, our meson-meson potentials have a form:

$$V_l^{c'c}(p'p|z) = V_l^{(nopole)c'c}(p'p|z) + \frac{\gamma^{c'}(p')\gamma^c(p)}{z - m_\alpha^0}. \tag{3.27}$$

These potentials have a pole at $z = m_\alpha^0$ (on the real z axis). To determine the T-matrix, $T_l^{c'c}(p'p|z)$, we need the renormalization procedure. Firstly we determine $T_l^{(nopole)c'c}(p'p|z)$ with only $V_l^{(nopole)c'c}(p'p|z)$ by solving

$$T_l^{(nopole)c'c}(p'p|z) = V_l^{(nopole)c'c}(p'p|z) + \sum_{c''} \int p''^2 dp'' \tag{3.28}$$

$$\times V_l^{(nopole)c'c''}(p'p''|z) \frac{1}{z - \omega_{p''}^{c''} + i\varepsilon} T_l^{(nopole)c''c}(p''p|z) \tag{3.29}$$

and define

$$\widetilde{\gamma}^c(p) = \gamma^c(p) + \sum_{c'} \int p'^2 dp' T_l^{(nopole)cc'}(pp'|z) \frac{1}{z - \omega_{p'}^{c'} + i\varepsilon} \gamma^{c'}(p') \tag{3.30}$$

$$\Sigma(z) = \sum_c \int p^2 dp \widetilde{\gamma}^c(p) \frac{1}{z - \omega_p^c + i\varepsilon} \gamma^c(p) \tag{3.31}$$

Then, we obtain

$$T_l^{c'c}(p'p|z) = T_l^{(nopole)c'c}(p'p|z) + \frac{\widetilde{\gamma}^{c'}(p')\widetilde{\gamma}^c(p)}{z - m_\alpha^{phys}(z)} \tag{3.32}$$

where $m_\alpha^{phys} = m_\alpha^0 + \Sigma(z)$

3.5 Resonances and compositeness

The resonance is one of the most prominent phenomena in the whole range of scattering experiments. Resonances observation in atomic, nuclear and particle physics mean that we search for the sharp peaks in the total cross section as a function on energy E_R with the width Γ to obtain the pole position $E = E_R - i\frac{\Gamma}{2}$. We approach the problem of resonance by the analytic properties of the amplitude scattering. We know that the poles of the S-matrix S_l in the upper half plane $\mathrm{Im}(\sqrt{s}) > 0$ correspond to the bound states of angular momentum l. In the other word, bound states correspond to the poles on positive imaginary axis, here we need to note that the virtual state correspond to the pole on negative imaginary axis. And resonances of angular momentum l appropriate to the pole on the unphysical sheet, that is, positive-real and negative imaginary region.

To find resonance poles, we calculate the S-matrix on complex E-plane. In principle, this is very simple, that is, we can extend z (total energy variable) to complex plane $z = \sqrt{s} = E_R + iE_I$ ($E_I < 0$). But in couple channel problems, we have many Riemann sheets. In our calculations, we searched resonance poles on the physical sheets ($ImP_c >$ 0)for closed channels and the unphysical sheets ($ImP_c <$0) for open channels.

In the paper of Tetsuo Hyodo [12] submitted in 2012, the author gives us the definition of compositeness in a single-channel chiral unitary approach as follow:

The compositeness of a bound state using the field renormalization constant which is given by the overlap of the bare state and the physical state in the nonrelativistic quantum mechanics, or by the residue of the bound state propagator in the relativistic field theory. The field renormalization constant enables one to define a normalized quantitative measure of compositeness of the bound state.

Hyodo's definition of compositeness is

$$\begin{aligned} \sum X_i &= 1 - Z && \text{: compositeness} \\ \Delta(z) &= \frac{Z}{z - M} && \text{: full Green function} \\ \Delta_0(z) &= \frac{1}{z - M_0} && \text{: free Green function} \end{aligned}$$

where

$$M = M_0 + g_0^2 G(M) \tag{3.33}$$

$$Z = [1 - g_0^2 G'(M)]^{-1} \tag{3.34}$$

and $G(z)$ is the (unrenormalized) loop function.

Applying this scheme to the coupled-channel of the meson-meson interaction in one-meson-exchange model, we define the compositeness of two-body resonances.

As mentioned in previous section, in the case with s-channel exchange potential the T-matrix is given by

$$T = T_{t,n} + \frac{\tilde{\gamma}(q_f)\tilde{\gamma}(q_i)}{\sqrt{s} - M^{phys}} \tag{3.35}$$

where,

$$\sqrt{s} - M_0 - \Sigma(\sqrt{s}) = \sqrt{s} - M^{phys} - \Sigma'(M^{phys})(\sqrt{s} - M^{phys}) \tag{3.36}$$

and $M^{phys} = M_0 + \Sigma(M^{phys})$. So, we have

$$\sqrt{s} - M_0 - \Sigma(\sqrt{s}) = [1 - \Sigma'(M^{phys})](\sqrt{s} - M^{phys}) \tag{3.37}$$

Since the field renormalization constant Z is the residue of the full's Green function, the compositeness in our model is defined by

$$1 - Z = 1 - \frac{\tilde{\gamma}(q_f)\tilde{\gamma}(q_i)}{\gamma(q_f)\gamma(q_i)} \left[1 - \Sigma'(M^{phys})\right]^{-1} \tag{3.38}$$

We introduce the residue matrix $R_{c'}(E_p)R_c(E_p)$ at the resonance energy E_p (on the complex E plane), which will be discussed in section 4.5.

$R_c(E_p)$ is defined by

$$S_{c'c} = i\frac{R_{c'}(E_p)R_c(E_p)}{E - E_p} + S_{c'c}^{(nopole)}(E) \tag{3.39}$$

In the case of the pole arising from s-channel meson-exchange diagram, $R_c(E_p)$ can be expressed by

$$R_c(E_p) = \frac{1}{4\pi}\sqrt{\frac{q_c}{E_p}}\widetilde{\gamma}_c(q_c)\left[1 - \frac{\partial\Sigma}{\partial E}(E_p)\right]^{-\frac{1}{2}} \tag{3.40}$$

$|R_c(E_p)|^2$ is a measure of the strength of coupling of the resonance to the channel c.

This page is intentionally left blank.

Chapter 4

Results and discussions

In this chapter, we show the results of the fit of the $\pi\pi - K\bar{K} - \pi\eta - \eta\eta$ and $\pi K - \eta K$ scattering to the most recent energy-dependent phase shift analyses at low and intermediate energy region based on the $SU(3)$-symmetric one-meson-exchange model. Some results of the renormalization procedure for the s-channel diagrams are given as the resonances. The resonances $f_0(980)$, $\rho(770)$, $a_0(980)$, $\sigma_1(400)$, $\sigma_2(600)$, $\phi(1020)$, $\kappa(1450)$, $\kappa(700)$ and $K^*(982)$ are determined by the S-matrix calculations on the complex E-plane. In $\pi\pi$ scattering at isospin $I = 0$, S-wave we found the existence of two poles of σ.

4.1 Parameters

Before discussing the results of meson-meson scattering, we show the results of numerical values of the parameters coupling constants, physical mass, and cut-off parameters. We use 24 free parameters to fit the meson-meson scattering phase shift analyses data. They consist of 5 coupling constants (g), 12 cut-off masses (Λ) and 7 bare masses (m_0). Since the model have two kinds of form factors, each of ones needs to be fitted separately. Therefore we have two set of parameter values for monopole and Gaussian form factors. All the parameters determined so as to reproduce $\pi\pi - K\bar{K} - \pi\eta - \eta\eta$ and $\pi K - \eta K$ scatterings are given in Table 4.1 and 4.2. It is difficult to fit with a large number of experimental data for all phase shift, specially for both well-fitting of $I = J = 0$ and $I = \frac{1}{2}, J = 0$. This means that it is hard to search a suitable values for the common parameters of t-channel for $\pi\pi$ and πK scattering. All coupling constants in vector meson-exchange diagrams are interrelated to the $\pi\pi\rho$ coupling by $SU(3)$-symmetry. Others involving the scalar (ϵ, κ) and tensor (f_2) mesons are independently adjusted to the data.

4.2 $\pi\pi - K\bar{K} - \pi\eta - \eta\eta$ scattering

In this section, we investigate the coupled-channel $\pi\pi - K\bar{K} - \pi\eta - \eta\eta$ scattering. In Fig. 4.1 - 4.4, we show the results of phase shifts δ_J^I ($I =$ isospin, $J =$ angular momentum)

Table 4.1: *Parameters.*

	Monopole	Gaussian
$g_{\pi\pi\rho}$	0.52295	0.50295
$g_{\pi\pi f_2}$	0.02865867	0.04697929
$g_{\pi\pi\epsilon_1}$	0.01620557	0.07761784
$g_{\pi\pi\kappa}$	0.3797329×10^{-3}	0.2302901×10^{-3}
$g_{K\bar{K}a_0}$	0.04088028	0.04088028
$\Lambda_{\pi\pi\rho}$	2491.25491	1668.19538
$\Lambda_{\pi KK^*}$	2262.68271	2872.62685
$\Lambda_{K\bar{K}\rho}$	3172.05083	1594.03348
$\Lambda_{K\bar{K}\omega,\phi}$	4527.63271	4598.07964
$\Lambda_{\pi\pi\rho;s}$	3115.30627	4192.68265
$\Lambda_{\pi\pi f_2;s}$	1416.81231	1960.48271
$\Lambda_{\pi\pi\varepsilon_1;s}$	1302.97135	1000.01549
$\Lambda_{\pi KK^*;s}$	4540.43306	4563.61723
$\Lambda_{\pi K\kappa;s}$	3282.23381	2725.66981
$\Lambda_{\eta KK^*}$	864.08419	864.08419
$\Lambda_{K\bar{K}a_0}$	1233.61523	1233.61523
$\Lambda_{K\bar{K}\phi}$	2137.02377	2137.02377

Table 4.2: *Parameters.*

M_0	Monopole	Gaussian
ρ	122.29105	1539.13199
ε_1	3799.83581	1559.90422
K^*	1530.82207	1453.16
κ	1557.59726	1892.54295
f_2	1354.23989	1892.54295
a_0	1235.73076	1280.73076
ϕ	1150.23241	1108.23241

in $\pi\pi$ scattering, comparing with the experimental data. In $I = 0, J = 0$ state, t-channel ρ, K^*, ϕ, ω-meson exchange and s-channel ϵ-meson exchange diagrams contribute to the interactions. In Fig. 4.1, we find a resonance pole at near $E = 980$ MeV. This resonance corresponds to the resonance in $\pi\pi$ scattering.

In our model, this resonance is interpreted as a quasi bound state of $\bar{K}K$ with binding energy $E \sim 10$ MeV and width $\Gamma \sim 40$ MeV (with monopole form factor) and ~ 300 MeV (with Gaussian form factor) (discussed later). This interpretation is very similar to that by D. Lohse et al. [10]. This resonance is produced by the strongly attractive $\bar{K}K$ interaction from t-channel vector (ρ, ω, ϕ) meson exchange diagrams. However, the s-channel ϵ-exchange potential is not important to forming of f_0 resonance. On the other hand, in this partial wave, the phase shifts are very difficult to deal with the experimental data. The derivative coupling increases strongly with the pion momentum above 1 GeV and gives a sharp rise to a potential which hardly change when the pion momentum below 1 GeV. When we adjust carefully the ϵ_1 meson with the coupling constant, the cut-off mass and the bare mass, good agreement between theory and experiment is obtained throughout the whole energy range. The bare mass and the coupling constant of ϵ_1 meson has been chosen to reproduce the phase shift in the high energy region. As a result, both the strongly attractive $K\bar{K}$ interaction and the ϵ_1 meson are necessary to get the agreement with the experiment.

Another very interesting point in this partial wave is the existence of two poles of $\sigma(\sigma_1, \sigma_2)$ at low energy region ($\sqrt{s} < 800$ MeV). These poles will be discussed in detail in section 4.5.

The one-meson-exchange diagrams which construct the potential of the isospin $I = 0$ total angular momentum $J = 2$ state, are almost the same with those ones in the momentum $J = 0$ states accept the mechanism of s-channel diagrams. There are 3 diagrams for s-channel with f_2 meson exchange, that is, $\pi\pi \to \pi\pi$, $K\bar{K} \to K\bar{K}$ and $\eta\eta \to \eta\eta$. The phase shifts in the isospin $I = 0$, D-wave state is shown in Fig. 4.3. The phase shift δ_2^0 is well-fitted with the experimental data both in monopole and Gaussian form factors. The s-channel with f_2 meson exchange make the phase shift more attractive and fitted with the experimental data by fitting the physical mass of f_2 resonance in $\pi\pi$ scattering.

The $I = 1$, P-wave potential in $\pi\pi - K\bar{K} - \pi\eta$ interactions is formed from the t-channel $\rho, \omega, \varphi, K^*$ exchange diagrams and the s-channel ρ exchange diagram. The latter diagram produces the ρ resonance at around $E = 800$ MeV in $\pi\pi$ scattering are shown in Fig. 4.4. In this partial wave, the ρ-meson exchange gives very important contribution both in the s- and t-channel exchange mechanisms, especially the s-channel ρ meson exchange dominates the strong attraction in $I = 1$, P-wave $\pi\pi$ interaction. The calculated phase shift is rather easy to fit with the experimental data. These good agreement of theoretical results with the experimental data in the phase shifts are obtained both in cases of the

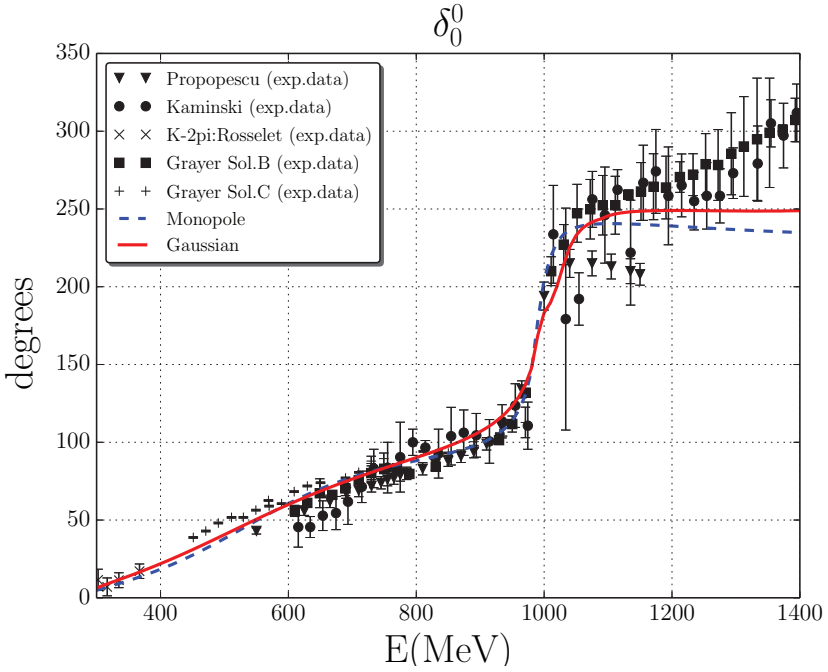

Figure 4.1: *Phase shift δ_0^0. The dashed blue line is the result with conventional monopole form factors. The solid red line is with the Gaussian form factor. The experimental phase shift analyses are taken from [13–16].*

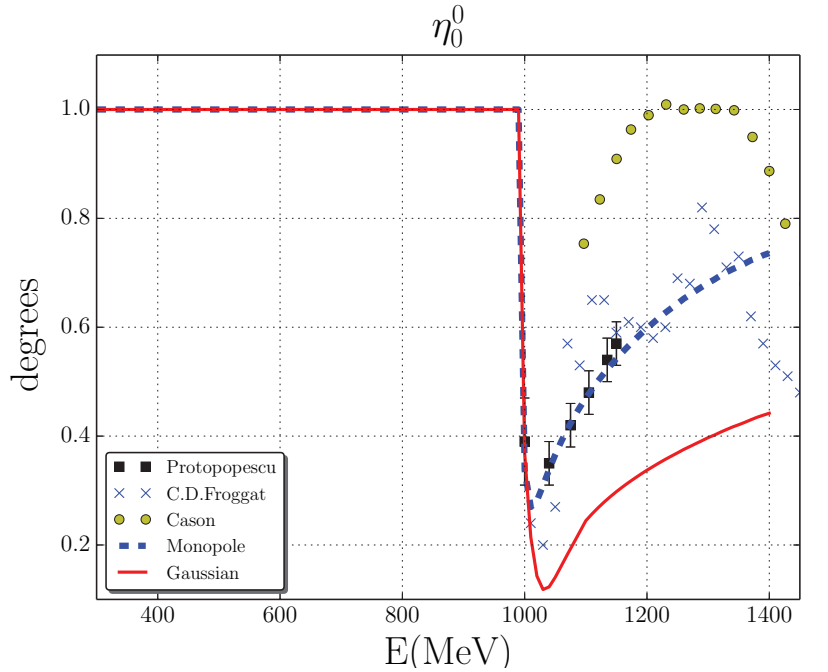

Figure 4.2: *Elasticity in the $I = J = 0$ $\pi\pi$ channel η_0^0. The dashed blue line is the result with conventional monopole form factors. The solid red line is with the Gaussian form factors. The experimental phase shift analyses are taken from Refs. [13, 17, 18].*

monopole and the Gaussian form factors.

In the $I = 0$, P-wave scattering, $\pi\pi$ and $\rho\rho$ channels are forbidden by the selection rule for identical bosons state. In this partial wave, therefore, $\bar{K}K$ single channel scattering

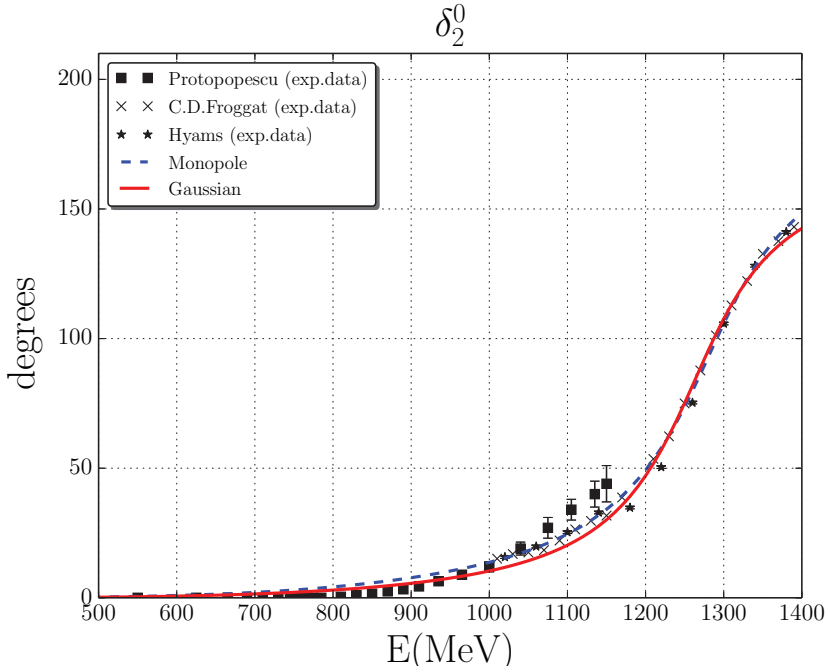

Figure 4.3: *Phase shift δ_2^0. The dashed blue line is the result with conventional monopole form factors. The solid red line is with the Gaussian form factors. The experimental phase shift analyses are taken from Refs. [13, 17, 19].*

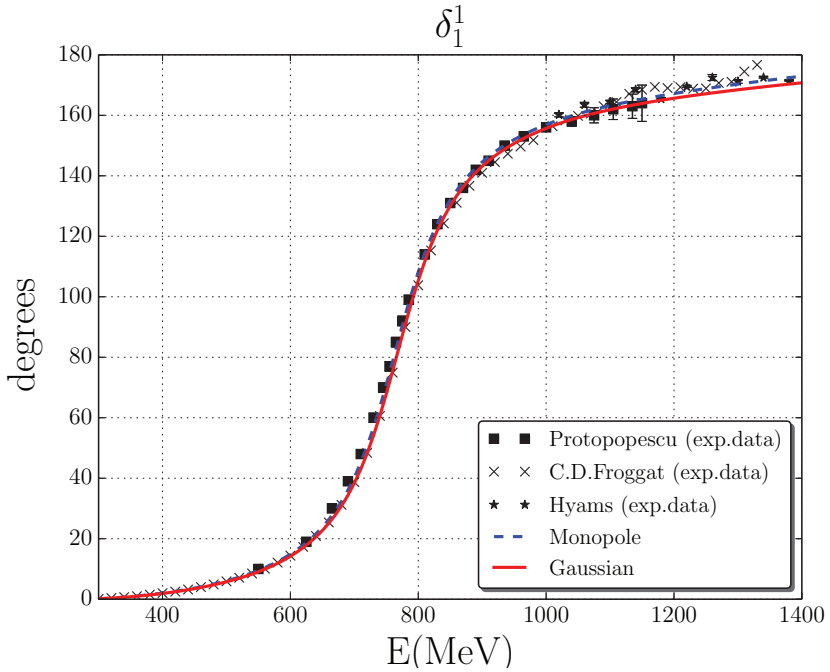

Figure 4.4: *Phase shift δ_1^1. The dashed blue line is the result with conventional monopole form factors. The solid red line is with the Gaussian form factors. The experimental phase shift analyses are taken from Refs. [13, 17, 19].*

occurs and the s-channel exchange diagrams with ω and ϕ dominate the attractive phase shifts. At present we have not found the experimental data to fit the phase shift at the $I = 0$, P-wave state. The phase shift of this partial wave is shown in Fig. 4.5. In

this figure, we see that the phase shifts only raise at the energy from 1 GeV to 1.040 GeV. When the energy is above 1.040 GeV, the phase shifts are almost the same. This phenomena propose us the role of s-channel with φ and ω meson exchange to form φ resonance in $K\bar{K}$ scattering.

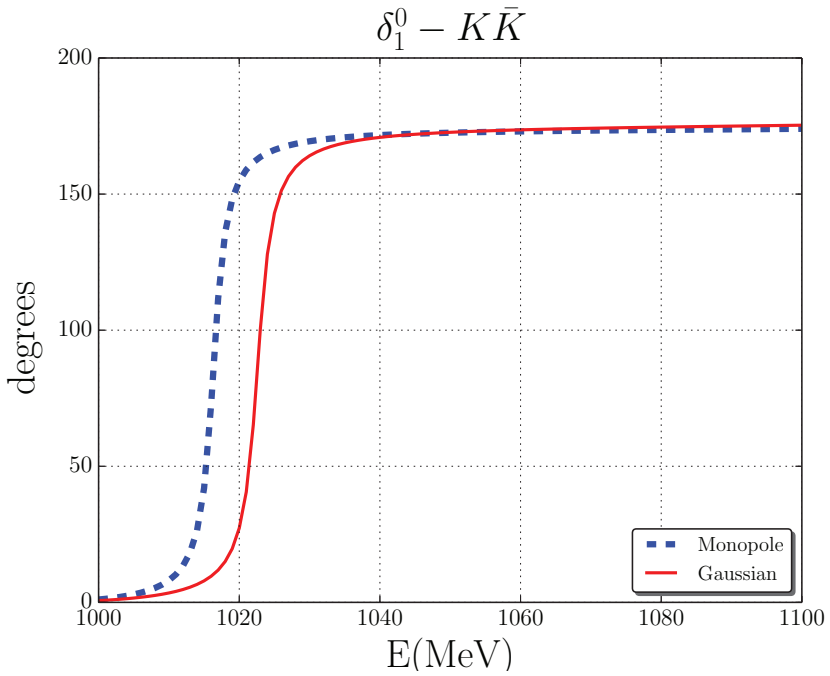

Figure 4.5: *Phase shift δ_1^0. The dashed blue line is the result with conventional monopole form factors. The solid red line is with the Gaussian form factors.*

The $I = 1$, S-wave potentials are constructed from $\rho, \omega, \varphi, K^*$ and a_0 meson exchange diagrams. The s-channel exchange with a_0 meson in the $K\bar{K} \to K\bar{K}$ and $\eta\eta \to \eta\eta$ reactions produces a_0 resonance in $\pi\eta$ scattering. The attractive phase shifts in this partial wave are shown in Fig. 4.6. There are no experimental data to fit with the calculated phase shifts.

When we treat the $I = 2$, S- and D- waves, the phase shifts of those are repulsive. These $I = 2, J = 0$ and $I = J = 0$ states describe a simple one-channel of $\pi\pi$ scattering with ρ meson exchange. The $I = 2, J = 0$ phase shifts are strong repulsive while the $I = J = 2$ ones are weak repulsive. The $I = J = 2$ phase shifts are weak repulsive because this state definitely requires the t-channel ρ exchange.

4.3 $\pi K - \eta K$ scattering

In the $\pi K - \eta K$ interaction, the t-channel ρ, K^* exchange diagrams and the s-channel κ (only in $I = \frac{1}{2}$, S-wave), K^* (only in $I = \frac{1}{2}$, P-wave) exchange diagrams are relevant. In this section, we only emphasize in the potential of the $I = \frac{1}{2}$ states because in these states we obtain attractive phase shifts and resonances. The repulsive phase shifts of

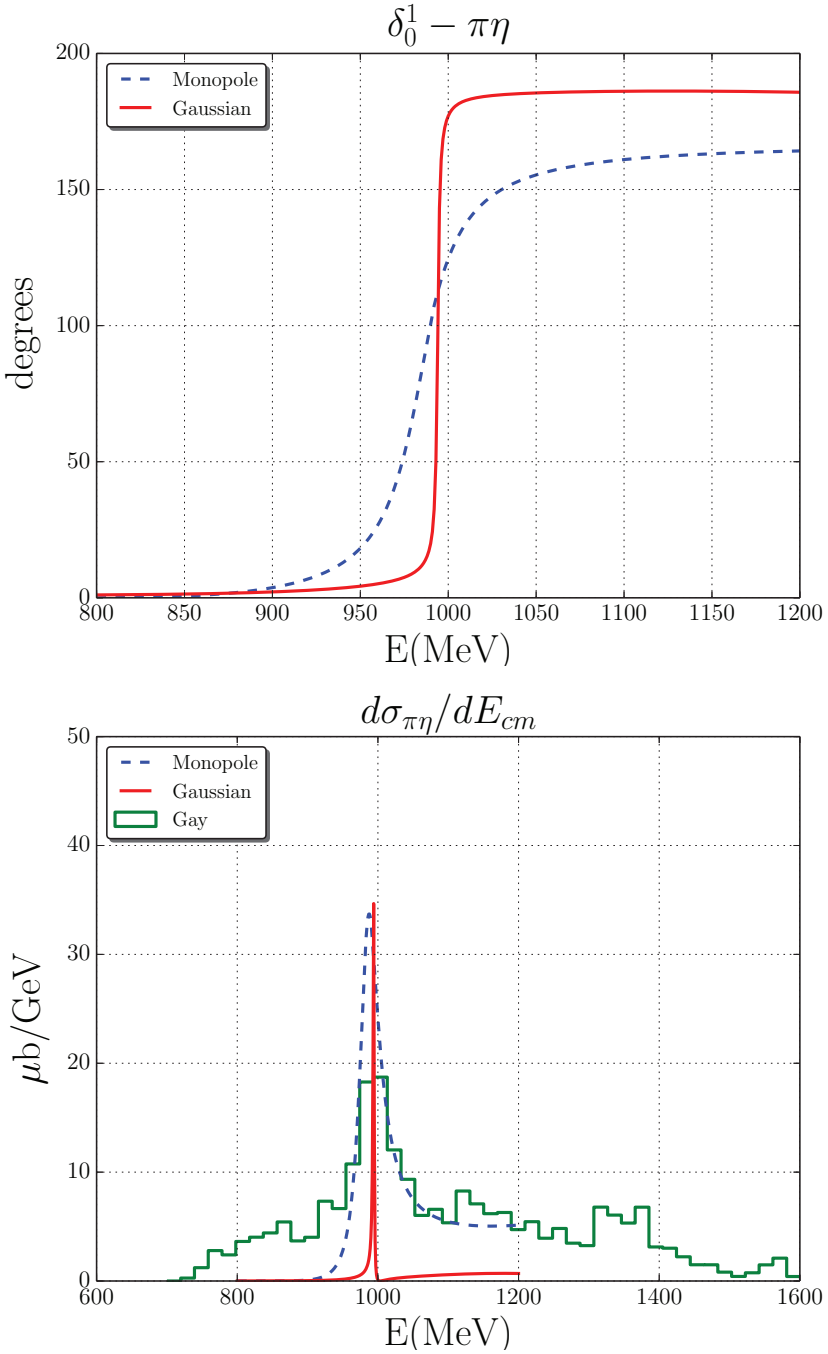

Figure 4.6: *Phase shift δ_0^1 and cross section $d\sigma/dE_{cm}$. The dashed blue line is the result with conventional monopole form factors. The solid red line is with the Gaussian form factors. The experimental $\pi\eta$ cross section analyses are taken from Refs. [20].*

the $I = \frac{3}{2}$ states are detail discussed in [22]. Moreover, by investigating the coupled-channel $\pi K - \eta K$ interactions, we understand the role of η meson in the meson-meson interactions by the one-meson-exchange model. Almost all of the parameters using in the $\pi K - \eta K$ interactions are determined from the previous investigation of $\pi\pi - K\bar{K} - \pi\eta - \eta\eta$ interactions and the $SU(3)$-symmetry relations. The t-channel exchange contributions are completely determined by the coupled-channel $\pi\pi - K\bar{K} - \eta\pi - \eta\eta$ interactions, whereas

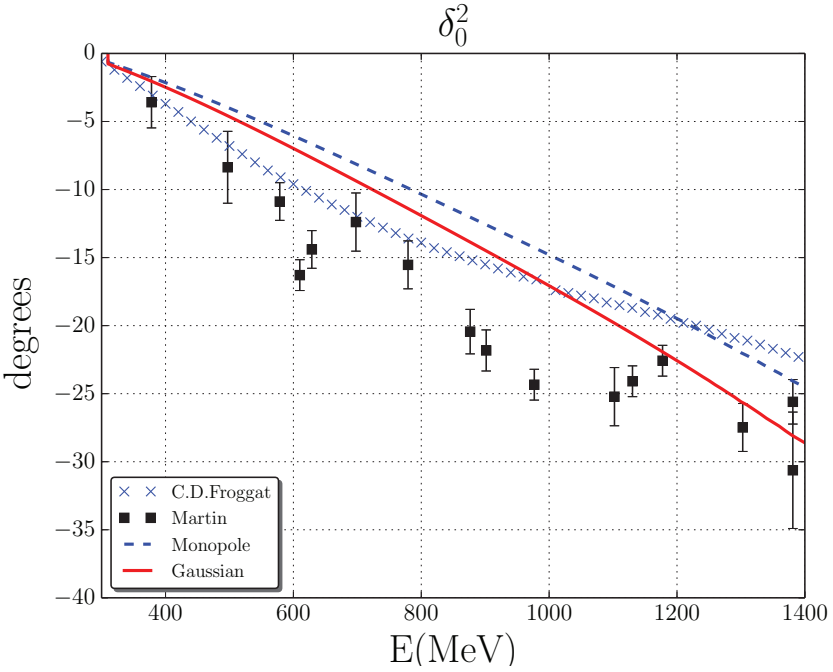

Figure 4.7: *Phase shift δ_0^2. The dashed blue line is the result with conventional monopole form factors. The solid red line is with the Gaussian form factors. The experimental phase shift analyses are taken from Refs. [17, 21].*

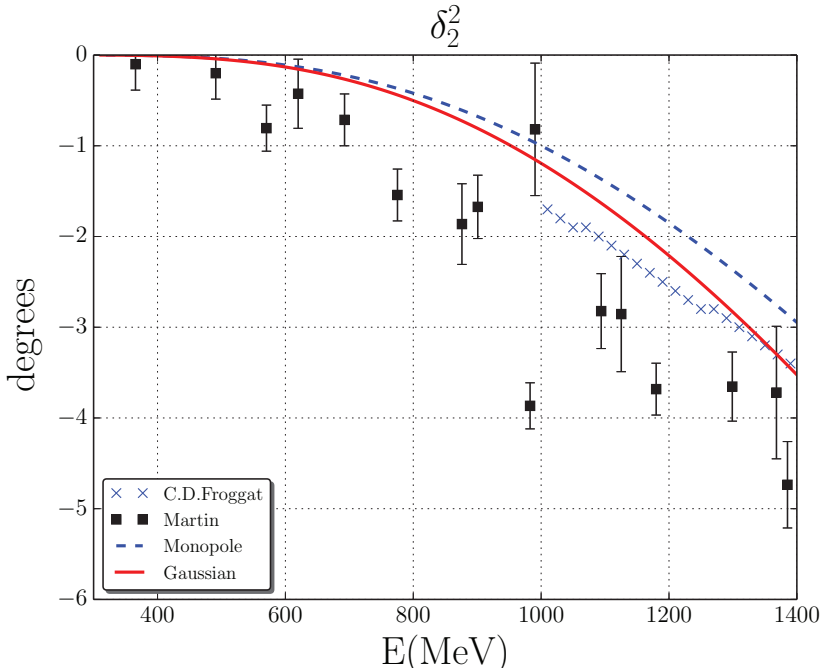

Figure 4.8: *Phase shift δ_2^2. The dashed blue line is the result with conventional monopole form factors. The solid red line is with the Gaussian form factors. The experimental phase shift analyses are taken from Refs. [17, 21].*

additional pole contributions in the s-channel with κ meson exchange have to be adjusted separately.

The phase shift $\delta_0^{\frac{1}{2}}$ of the $\pi K - \eta K$ system is attractive. As shown in Fig. 4.9, in the

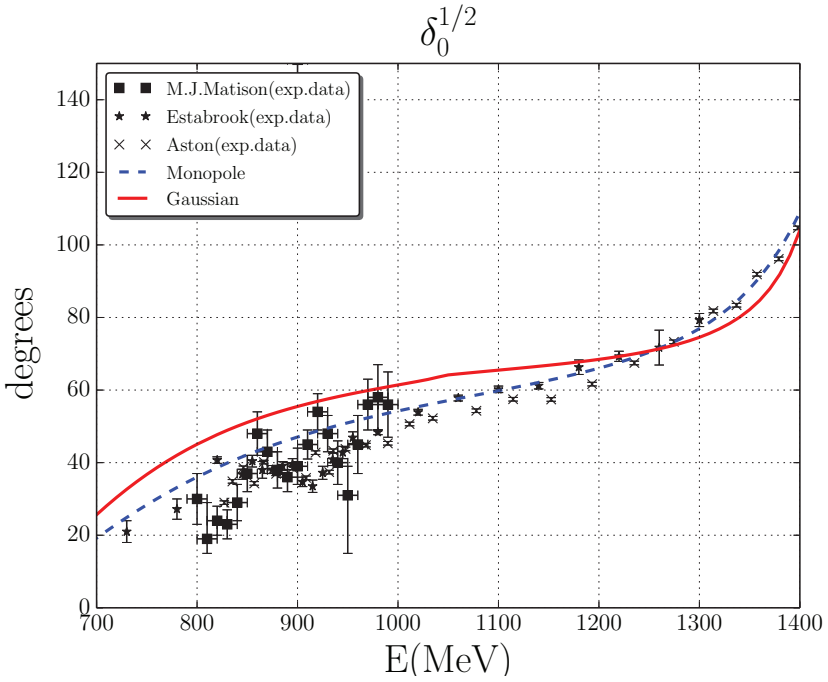

Figure 4.9: *Phase shift $\delta_0^{\frac{1}{2}}$. The dashed blue line is the result with conventional monopole form factors. The solid red line is with the Gaussian form factors. The experimental phase shift analysis are taken from Refs. [23–25].*

low-energy region ($\sqrt{s} < 1$ GeV), the calculated phase shifts are somewhat larger than the experimental ones. However, in the higher energy region, we find a good agreement with the experimental data. The calculated results with the monopole form factor give a better fit to the experimental data than that with the Gaussian form factors. Because some of the parameters in $\pi K - \eta K$ interactions have the influence of the one in $\pi\pi - K\bar{K} - \pi\eta - \eta\eta$ scatterings, therefore, it is rather hard to fit the phase shift well. By adjusting the parameters of the s-channel exchange diagram, we finally reach the rather good results of phase shift and the position of poles.

The strongly attractive phase shifts for the $I = \frac{1}{2}$, P-wave $\pi K - \eta K$ interaction are shown in Fig. 4.10. The agreement of the theoretical calculation with the experimental data are very good at the low-energies region ($E < 1$ GeV), however it is a little larger than experimental data at higher energies ($E > 1$ GeV). The resonance state in the $I = \frac{1}{2}$, P-wave scattering is shown in Fig. 4.10.

4.4 KK interaction

In this section, we extend our model to the $S = 2(KK)$ sector based on the flavor $SU(3)$-symmetry and predict the properties of the KK interaction in S-, P-, D- and F-waves. The KK interaction has only t-channel with ρ, ω and φ meson-exchange.

In Fig. 4.12 - 4.15, we propose the predictions for phase shifts δ_0^1, δ_1^0, δ_2^1 and δ_3^0. At the present, we have not found any experimental data to fit these phase shift. In $I = 1$,

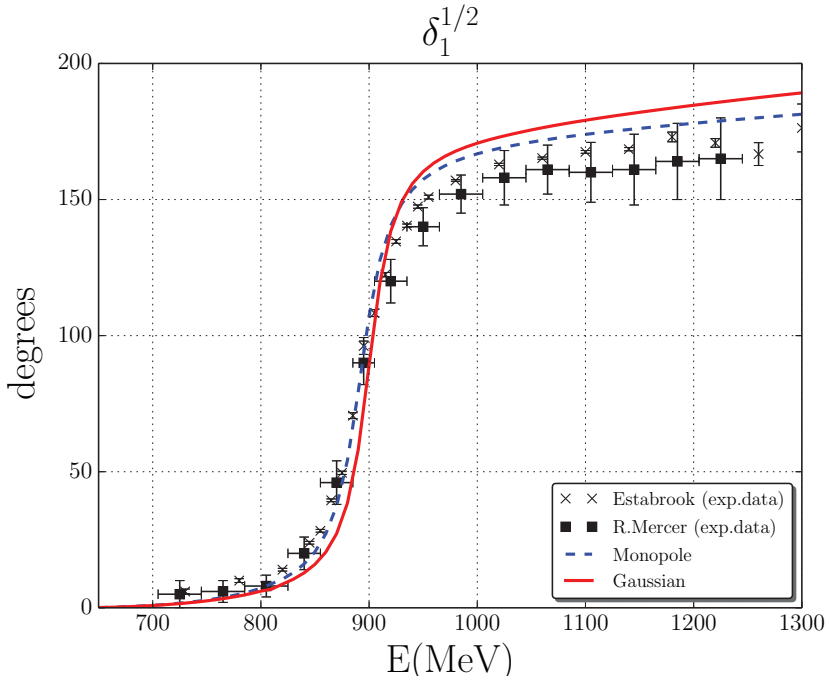

Figure 4.10: *Phase shift $\delta_1^{\frac{1}{2}}$. The dashed blue line is the result with conventional monopole form factors. The solid red line is with the Gaussian form factors. The experimental phase shift analyses are taken from Refs. [24] and [26].*

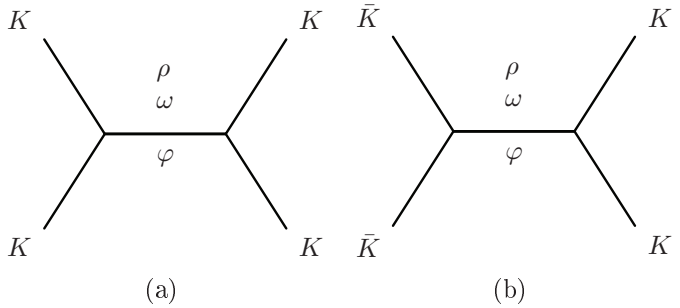

Figure 4.11: *t-channel exchange diagrams in our model of (a) KK interaction (b) $K\bar{K}$ interaction.*

S-wave, the phase shifts have large negative. This means that our KK interaction in this wave is strongly repulsive. On the other hand, in $I = 0$, P-wave, we obtain positive phase shifts which mean attractive interaction. By investigating the contributions from ρ, ω and φ meson exchanges, we can understand the mechanism of such behavior. With ρ meson exchange, the $I = 0$, KK interaction is attractive, while with ω and φ meson exchange, they are both repulsive. And with sum of these meson exchanges in the KK interaction, we obtain a weak attractive one (see Fig. 4.13). Otherwise, the same isospin state, $K\bar{K}$ interaction is very strong one (see detail in table 4.3 and 4.4). From the contributions of meson exchange in KK interaction, we can see the important role of ρ meson in meson exchange model. In $I = 1$ states, the vector meson ρ makes both KK and $K\bar{K}$ interactions repulsive. The ω and φ meson exchanges make the KK interaction

repulsive and make $K\bar{K}$ interaction attractive. Therefore, we get strongly repulsive KK interaction as a result of the sum of three meson exchange contributions.

Table 4.3: *Contributions from ρ, ω and φ meson exchanges in KK scattering.*

KK	ρ	ω	φ	ρ, ω, φ
$I = 0, J = 1$	attractive	repulsive	repulsive	attractive
$I = 1, J = 0$	repulsive	repulsive	repulsive	strong repulsive

Table 4.4: *Contributions from ρ, ω and φ meson exchanges in $K\bar{K}$ scattering.*

$K\bar{K}$	ρ	ω	φ	ρ, ω, φ
$I = 0, J = 0$	attractive	attractive	attractive	strong attractive
$I = 1, J = 1$	repulsive	attractive	attractive	attractive

The interaction in the $I = 1$, D-wave is predicted to be a weak repulsive one. We also have the prediction of F-wave KK interaction. This result shows that this interaction is weak attractive.

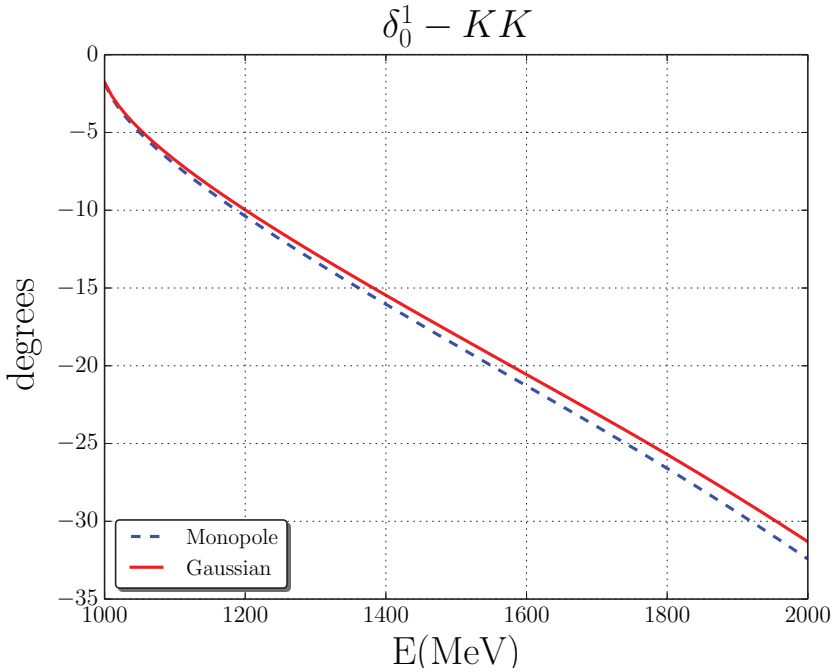

Figure 4.12: *Phase shift δ_0^1. The dashed blue line is the result with conventional monopole type form factors. The solid red line is with the Gaussian type form factor.*

A prominent feature of our predictions is an attractive $I = 0$, P-wave KK interaction. In fact, our model predicts positive phase shifts as shown in Fig. 4.13. Other physicist believed that in this channel of KK interaction, the phase shift is repulsive. All these result show that the relative strengths of ρ, ω and φ meson-exchange contributions are very important.

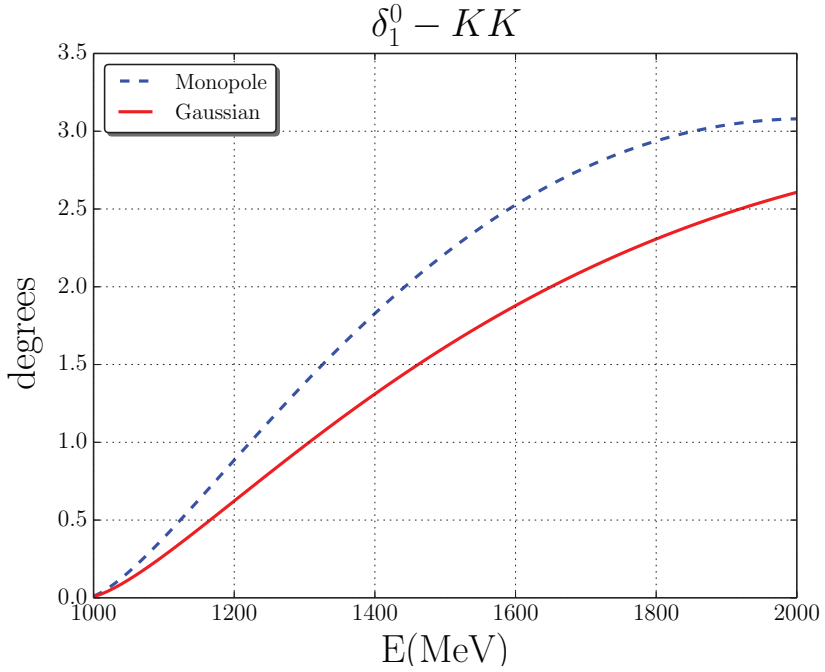

Figure 4.13: *Phase shift δ_1^0. The dashed blue line is the result with conventional monopole type form factors. The solid red line is with the Gaussian type form factor.*

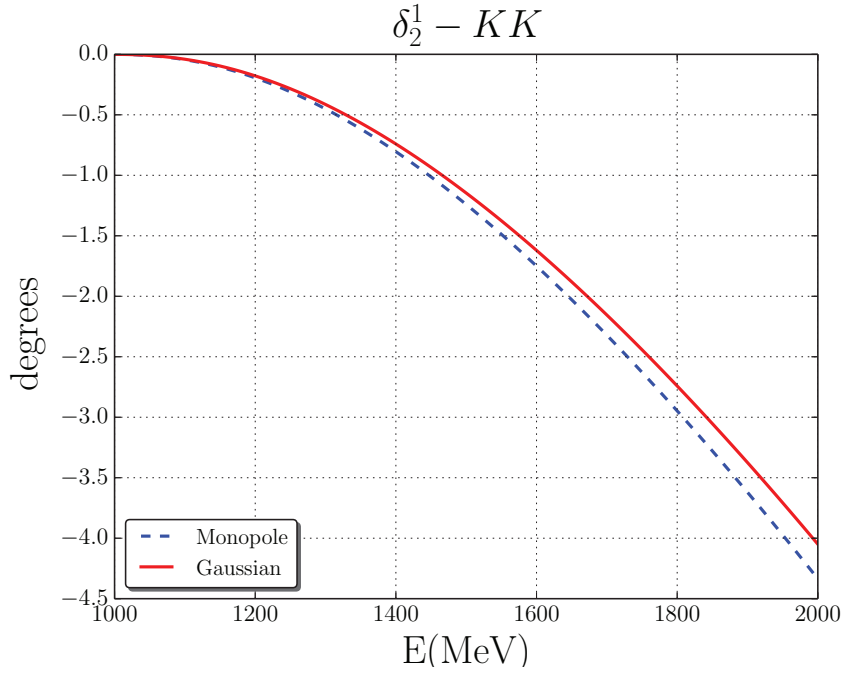

Figure 4.14: *Phase shift δ_2^1. The dashed blue line is the result with conventional monopole type form factors. The solid red line is with the Gaussian type form factor.*

4.5 Resonances

In this section, we propose the resonances in the $\pi\pi - K\bar{K} - \pi\eta - \eta\eta$ and $\pi K - \eta K$ scatterings. The formulation to calculate these resonances was shown in section 3.5 in the previous chapter. Therefore, we want to summarize the calculated results of resonance

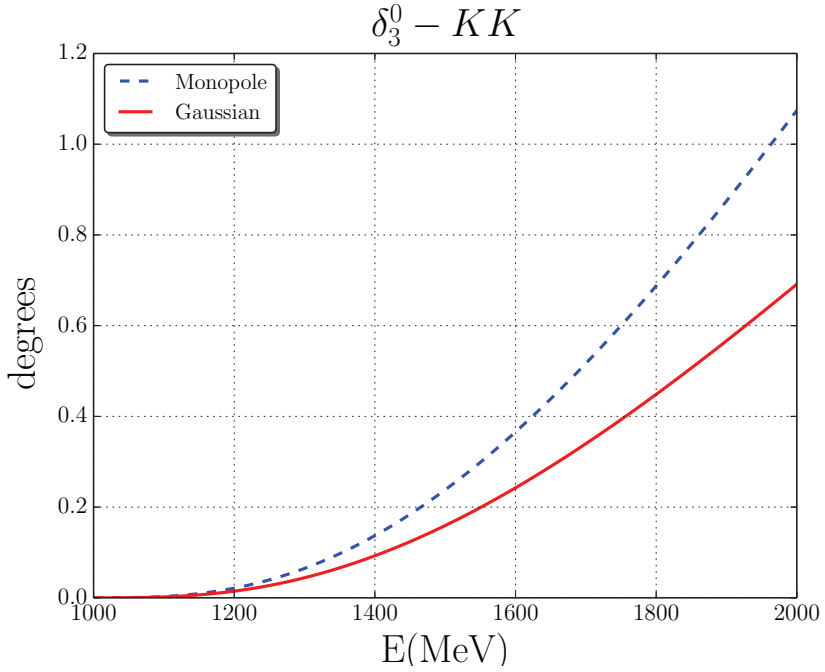

Figure 4.15: *Phase shift δ_3^0. The dashed blue line is the result with conventional monopole type form factors. The solid red line is with the Gaussian type form factor.*

poles in the meson-meson scattering in comparison with those in experiments. All the pole positions of the calculated and experimental resonances in $\pi\pi - K\bar{K} - \pi\eta - \eta\eta$ and $\pi K - \eta K$ scatterings are summarized in Tables 4.5 and 4.6, respectively.

There are 3 pole resonances of the coupled $\pi\pi - K\bar{K} - \eta\eta$ scattering at the $I = 0$, S-wave state, that is, $f = 0(980)$, $\sigma_1(400)$ and $\sigma_(600)$. The $f_0(980)$ have the physical mass $m = 1000$ MeV and the width $\Gamma = 40$ MeV for monopole form factor case (see Table 4.5). For the Gaussian case, we have the pole at the physical mass $m = 1075$ MeV and the width $\Gamma = 340$ MeV. We realize that the width of the resonance in the case of Gaussian form factor is too wide in comparison with the experiment data. In the case of monopole form factor, the ratio of residue matrix elements at the pole is $|R_{\pi\pi}|^2 : |R_{K\bar{K}}|^2 : |R_{\eta\eta}|^2 = 0.41 : 0.59 : 0.00$ for f_0 resonance, $0.98 : 0.017 : 0.002$ for σ_1 resonance, and $0.48 : 0.33 : 0.18$ for σ_2 resonance. These ratio means that there are two pure dynamical resonances at the $I = J = 0$ in the $\pi\pi - K\bar{K} - \eta\eta$ scattering, that is, $f_0(980)$ and $\sigma_1(400)$. The σ_2 resonance corresponds to pole by the s-channel epsilon exchange in the $\pi\pi - K\bar{K}$

Because of the well-reproduced $\pi\pi$ phase shifts of the $I = 0$, D-wave in the $\pi\pi - K\bar{K} - \eta\eta$ scattering, we determine the $f_2(1270)$ resonance rather exactly with the experiment data. This resonance is at $m = 1270$ MeV with the width of 220 MeV for monopole form factor case (see Table 4.5). For the Gaussian case, the resonance is at $m = 1250$ MeV with the width of 180 MeV. For the case of D-wave in monopole form factor, we have the ratio of residue matrix elements such as $|R_{\pi\pi}|^2 : |R_{K\bar{K}}|^2 : |R_{\eta\eta}|^2 = 0.66 : 0.27 : 0.07$. This

ratio shows that the f_2 resonance has only small coupling to $\eta\eta$ and considerably large couping (27%) to $K\bar{K}$ channel.

The agreement of theoretical results with the experimental data in phase shifts indicates that both the position and the width of the ρ meson are described very well both in monopole and Gaussian form factors. In fact, the resonance of the $I = J = 1$ is at $m = 800$ MeV with the width of 140 MeV for monopole form factor case (see Table 4.5). For the Gaussian form factor case, the resonance is at $m = 800$ MeV with the width of 120 MeV. For the case of P-wave with the monopole form factor, we have the ratio of residue matrix elements such as $|R_{\pi\pi}|^2 : |R_{K\bar{K}}|^2 : |R_{\pi\eta}|^2 = 0.67 : 0.0005 : 0.33$. This ratio shows that the ρ resonance has no $K\bar{K}$ component but 33% comes from the $\pi\eta$ component.

Table 4.5: *Resonance poles in the $\pi\pi - K\bar{K} - \eta\pi - \pi\pi$ scattering.*

	Experiment Data	Monopole	Gaussian
$f_0(980)$	$(970 - 1010) - i(20 - 50)$	$1000 - i20$	$1075 - i170$
σ_1	$(400 - 500) - i(200 - 350)$	$410 - i560$	$390 - i500$
σ_2	–	$580 - i360$	$430 - i380$
$a_0(980)$	$980 - i(25 - 50)$	$845 - i15$	$800 - i15$
$\rho(770)$	$775 - i74$	$800 - i60$	$800 - i60$
$\phi(1020)$	$1019 - i2.1$	$1016.5 - i1.6$	$1022.5 - i1.6$
$f_2(1270)$	$(1275 \pm 1.2) - i93$	$1270 - i110$	$1050 - i90$

With the strangeness $S = 0$, $I = 1$, S-wave, we have the a_0 resonance. This resonance is at $m = 845$ MeV with the width of 30 MeV for the monopole form factor case (see Table 4.5). For the Gaussian case, the resonance is at $m = 800$ MeV with the width of 30 MeV. For the case of monopole form factor, we have the ratio of residue matrix elements such as $|R_{\pi\eta}|^2 : |R_{K\bar{K}}|^2 = 0.14 : 0.86$. This ratio mean that the a_0 resonance has a large $K\bar{K}$ component.

The κ resonance with s-channel meson exchange of the $I = \frac{1}{2}$, S-wave in the $\pi K - \eta K$ scattering is also reproduced very well. The existence of two κ poles in the s-wave is very interesting point of the $\pi K - \eta K$ scattering. In the previous calculation of D.Lohse [10], they have not considered the ηK scattering. The fist pole of $\kappa(700)$ is a dynamical pole in the πK scattering. In our calculation, we investigate the coupling with the ηK channel, therefore, the second pole of κ maybe come from the interaction by the s-channel meson exchange diagrams. The corresponding physical mass of the meson scalar is $m_\kappa = 1450$ MeV with the width $\Gamma_\kappa = 150$ MeV for monopole form factor and $m_\kappa = 1440$ MeV with the width $\Gamma_\kappa = 70$ MeV in Gaussian form factor. For the case of monopole form factor, we have the ratio of residue matrix elements such as $|R_{\pi K}|^2 : |R_{\eta K}|^2 = 0.92 : 0.08$ for the $\kappa(1450)$ resonance and $|R_{\pi K}|^2 : |R_{\eta K}|^2 = 0.96 : 0.04$ for the $\kappa(700)$. These ratios show

that these resonances are dominated by the πK channels.

Table 4.6: *Resonance poles position of the $\pi K - \eta K$ scattering.*

	Experiment Data	Monopole	Gaussian
$\kappa(700)$	$(653 - 711) - i270$	$650 - i230$	$650 - i190$
$\kappa(1450)$	$(1375 - 1475) - i(95 - 175)$	$1450 - i75$	$1440 - i35$
K^*	$892 - i25$	$907 - i20$	$910 - i18$

The pole with s-channel meson exchange of the P-wave of the $\pi K - \eta K$ scattering reproduces well by the $K^*(892)$ resonance. In Table 4.6, we see that the physical mass of vector meson exchange is $m_{K^*} = 907$ MeV with the width $\Gamma_{K^*} = 40$ MeV for monopole form factor and $m_{K^*} = 910$ MeV, $\Gamma_{K^*} = 36$ MeV for Gaussian form factor. In comparison with the experiment data, the calculated pole position are a little shifted, but it is reasonable because of the not-well-fitting of the phase shifts $\delta_1^{\frac{1}{2}}$ at the high energy region ($E > 950$ MeV) as shown in Fig 4.10. For the case of monopole form factor, we have the ratio of residue matrix elements such as $|R_{\pi K}|^2 : |R_{\eta K}|^2 = 0.63 : 0.37$. This ratio shows that ηK component is not small in this resonance.

This page is intentionally left blank.

Chapter 5

Roles of η meson

In this chapter, we discuss the roles of η channels ($\pi\eta$, $\eta\eta$, ηK channels) in the $\pi\pi - K\bar{K} - \pi\eta - \eta\eta$ and $\pi K - \eta K$ scatterings. It should be no doubt that the roles of the η-meson are indispensable in these scatterings to have an adequate view of meson-meson interactions.

We define two models that we consider in this section, the model with η, which contains the $\pi\pi - K\bar{K} - \pi\eta - \eta\eta$ and $\pi K - \eta K$ interactions, and the model without η, which includes only the $\pi\pi - K\bar{K}$ and πK interactions.

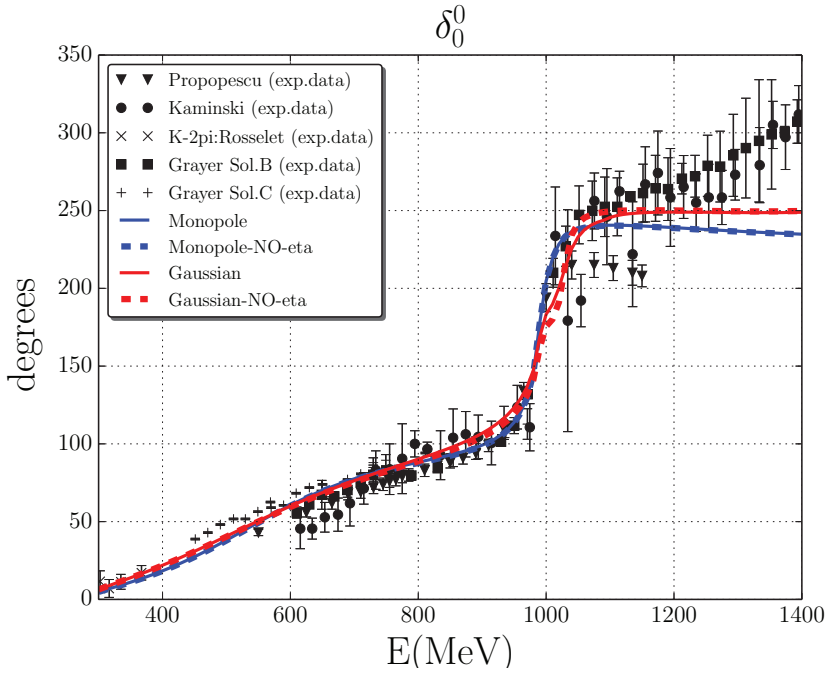

Figure 5.1: *Phase shifts δ_0^0 in the model with η. The solid blue line is the result with conventional monopole form factors. The solid red line is with the Gaussian form factors. The dashed lines are those in the model without η. The experimental phase shift analyses are taken from Refs. [13–16].*

When we keep the same parameter values with those given in Tables 4.1 and 4.2, the phase shifts of *the model with η* and *the model without η* are almost the same in both kinds of form factors except the phase shifts in the $I = 1$, S-wave (see Fig. 5.4).

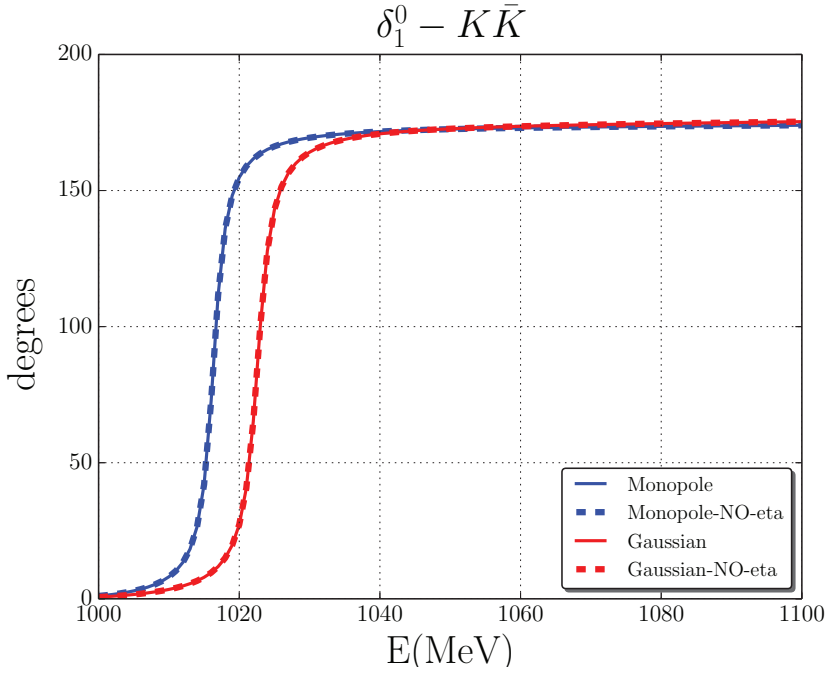

Figure 5.2: *Phase shifts δ_1^0 in the model with η. The solid blue line is the result with conventional monopole form factors. The solid red line is with the Gaussian form factors. The dashed lines are those in the model without η.*

In the $I = 1$, S-wave $\pi\eta - K\bar{K}$ scattering, we find a resonance pole corresponding to $a_0(980)$ resonance, as shown in Fig. 5.4. In the model with η (the $\pi\eta - K\bar{K}$ model), we find this resonance in the $\pi\eta$ phase shifts at the correct energy $E = 980$ MeV.

On the other hand, in the model without η (the single channel $K\bar{K}$ model), this resonance appears as a resonance in the $K\bar{K}$ phase shifts at $E = 1070$ MeV (in the case of the monopole factor), which is much higher than the a_0 resonance mass.

On the complex E-plane, this resonance pole is identified at $E = 845 - i15$ MeV (in the model with η) and $890 - i35$ MeV (in the model without η) as given in Table 5.1. This means that the resonance position defined by phase shifts on the real E-axis is much different from the pole of the S-matrix on the complex E-plane. Such very interesting behavior may be understood by the moving pole with the E-dependent interactions.

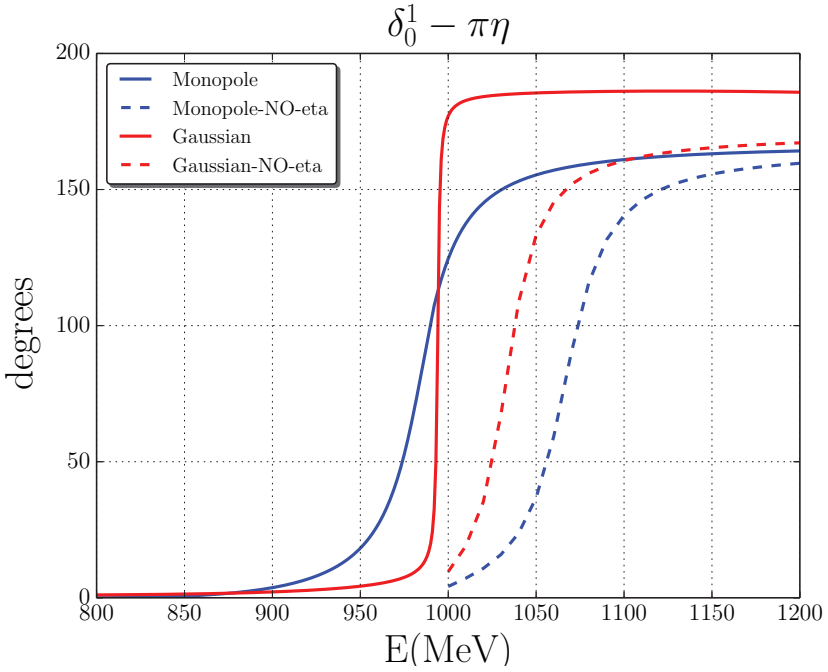

Figure 5.3: *Phase shifts δ_0^1 in the model with η. The solid blue line is the result with conventional monopole form factors. The solid red line is with the Gaussian form factors. The dashed lines are $K\bar{K}$ phase shifts in the model without η.*

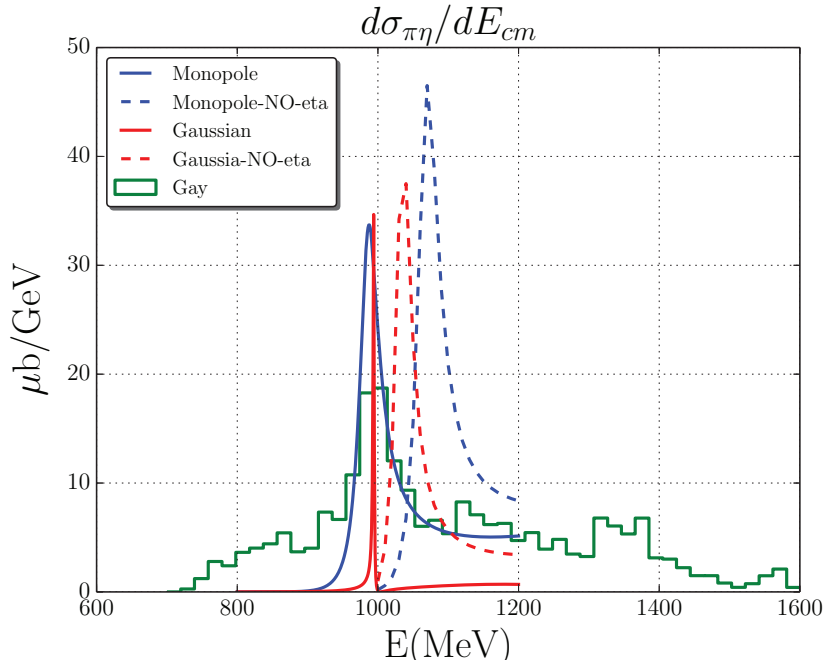

Figure 5.4: *The solid blue line is the result with conventional monopole form factors. The solid red line is with the Gaussian form factors. The dashed lines are the $K\bar{K}$ cross sections in the model without η. The experimental $\pi\eta$ cross sections are taken from Refs. [20].*

Table 5.1: *Resonance poles in the $\pi\pi - K\bar{K} - \pi\eta - \eta\eta$ scatterings.*

	Experiment Data	Monopole	Monopole-no η	Gaussian	Gaussian-no η
$f_0(980)$	$(970 - 1010) - i(20 - 50)$	$1000 - i20$	$1000 - i20$	$1075 - i170$	$1060 - i200$
σ_1	$(400 - 500) - i(200 - 350)$	$410 - i560$	$430 - i570$	$390 - i500$	$390 - i510$
σ_2	–	$580 - i360$	$560 - i360$	$430 - i380$	$430 - i390$
$a_0(980)$	$980 - i(25 - 50)$	$845 - i15$	$890 - i35$	$860 - i15$	$880 - i5$
$\rho(770)$	$775 - i74$	$800 - i70$	$800 - i70$	$800 - i60$	$800 - i60$
$\phi(1020)$	$1019 - i2.1$	$1016.5 - i1.6$	$1016.5 - i1.6$	$1022.5 - i1.6$	$1022.5 - i1.6$
$f_2(1270)$	$(1275 \pm 1.2) - i93$	$1270 - i110$	$1270 - i110$	$1050 - i90$	$1280 - i110$

Table 5.2: *Resonance poles in the $\pi K - \eta K$ scatterings.*

	Experiment Data	Monopole	Monopole-no η	Gaussian	Gaussian-no η
$\kappa(700)$	$(653 - 711) - i270$	$650 - i230$	$660 - i220$	$650 - i190$	$650 - i200$
$\kappa(1450)$	$(1375 - 1475) - i(95 - 175)$	$1450 - i75$	$1450 - i75$	$1440 - i35$	$1440 - i30$
K^*	$892 - i25$	$907 - i20$	–	$910 - i18$	–

When we compare the phase shifts in the two models for the $\pi K - \eta K$ scattering, we realize that there are a large change in the phase shifts in the $I = \frac{1}{2}$, P-wave (see the Fig. 5.6). This means that the η channel has a large effect in this P- wave. It is reasonable that the pole position of K^* do not exist at the same calculated region, it was shifted to the higher energy region. The detail values of pole positions are shown in Table 5.2 to compare its in the two models.

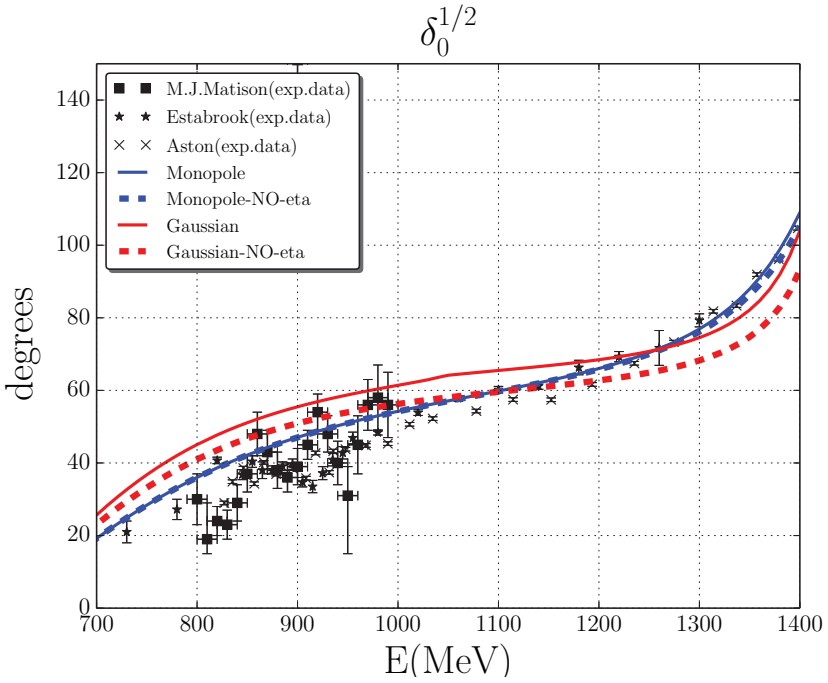

Figure 5.5: *Phase shifts $\delta_0^{\frac{1}{2}}$ in the model with η. The solid blue line is the result with conventional monopole form factors. The solid red line is with the Gaussian form factors. The dashed lines are those in the model without η. The experimental phase shift analyses are taken from Refs. [23–25].*

As a brief summary, we see that the η channels play very important and necessary roles in the full treatment of the meson-meson interaction by one-meson-exchange mechanisms. The $\eta\eta$ channel has a small effect in coupling to the $\pi\pi - K\bar{K}$ scattering, while the $\pi\eta$ channel has a large effect to the $K\bar{K}$ channel. The η channel contributed to the appearance of a_0 resonance in the $\eta\pi$ interaction. In the the $I = \frac{1}{2}$, P-wave for the πK scattering, the η channel also has a part in producing the well-fitted phase shifts.

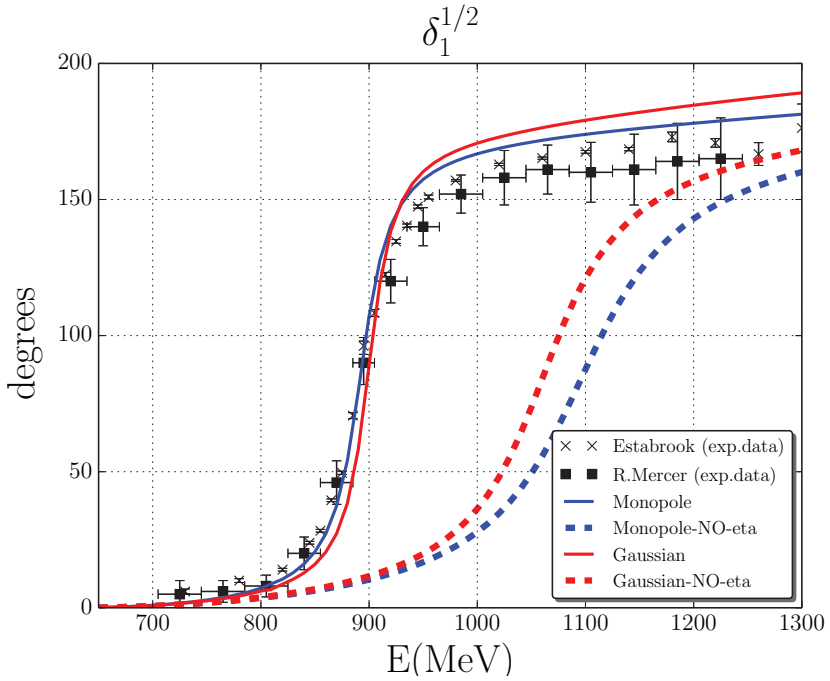

Figure 5.6: *Phase shifts $\delta_1^{\frac{1}{2}}$ in the model with η. The solid blue line is the result with conventional monopole form factors. The solid red line is with the Gaussian form factors. The dashed lines are those in the model without η. The experimental phase shift analyses are taken from Refs. [24, 26].*

Chapter 6

Conclusion

In the purpose of description of hadron-hadron interactions in a unified way, we constructed the one-meson-exchange potential model of the meson-meson interactions based on the interaction Lagrangian which satisfies the $SU(3)$-symmetry. In order to determine parameters in the potential, which include two kinds of form factors (monopole and Gaussian) and coupling constants, we used the phase shift data of $\pi\pi$ and πK scatterings at low energies. The results of the fit of the $\pi\pi - K\bar{K} - \pi\eta - \eta\eta$ and $\pi K - \eta K$ scatterings are reproduced to the most recent energy-dependent phase shift analyses at low and intermediate energy region based on the $SU(3)$-symmetric one-meson-exchange model. The quantitative phase shifts of the KK interaction are determined by extending the $\pi\pi - K\bar{K} - \pi\eta - \eta\eta$ and $\pi K - \eta K$ scatterings. In the KK interaction, t-channel ρ, ω and ϕ meson exchange plays an important role.

We know that the resonance is one of the most prominent phenomena in the whole range of scattering experiments. We approach the problem of resonance by the analytic properties of the amplitude scattering of meson-meson interactions. Beside the well-reproduced poles of pure dynamical resonance f_0(980 at the isospin $I = 0$, S-wave we also found the existence of the other pure dynamical pole position of σ_1 and the σ_2, which come from the s-channel ϵ exchange diagram. By calculating the ratio of residue matrix elements at the poles, we understand that the σ_1 and σ_2 have much different character. Moreover, by using Haftel-Tabakin method to deal with the singularity of the Green function of the scattering amplitude, we obtained the numerical calculations of the physical masses and the width of the pole positions of $\pi\pi - K\bar{K} - \pi\eta - \eta\eta$ and $\pi K - \eta K$ scattering, that is, $\rho(770)$, $a_0(980)$, $\phi(1020)$ $f_2(1270)$, $\kappa(700)$, $\kappa(1430)$ and $K^*(892)$ resonances. We also have two pole position of κ of the $\pi K - \eta K$ scattering at the isopin $I = \frac{1}{2}$, S-wave. In this dissertation, we also give a brief introduction to the compositeness of the two-body resonances.

In addition, the $\pi\pi - K\bar{K} - \eta\eta$ and $\pi K - \eta K$ interactions also have been discussed to investigate the role of η meson in the $\pi\pi$ and πK scatterings. The $\eta\eta$ channel has a small effect in coupling to the $\pi\pi - K\bar{K}$ scattering, while the $\pi\eta$ channel has a large

effect to the $K\bar{K}$ channel. The η channel contributed to the appearance of a_0 resonance in the $\eta\pi$ interaction. In the $I = \frac{1}{2}$, P-wave η channel also has a part in producing the well-fitted phase shifts.

In the future, we will refine the meson-meson interaction ($\pi\pi - \pi\bar{K} - \pi\eta - \eta\eta$ and $\pi K - \eta K$) by the meson-exchange model. We may make the more well-fitted parameter set to well-reproduce the phase shift δ_0^0 and $\delta_0^{\frac{1}{2}}$, especially in the case of Gaussian form factors. We also would like to investigate the field normalization to understand the quantitative measure of compositeness of the two-body resonances. After that, we would like to advance forward by solving the three-body problems to study the existences and properties of the resonances in the hadronic systems.

Appendix A

The flavor SU(3) model of hadrons and hadron interaction

A.1 The flavor SU(3) model of hadrons

The extension from SU(2) to SU(3) is immediate if we extend the basic u, d doublet to triplet u, d, s and investigate transformations of

$$\phi \equiv \begin{pmatrix} \mathrm{u} \\ \mathrm{d} \\ \mathrm{s} \end{pmatrix}$$

of the form

$$\phi' = U\phi$$

where U is now a 3×3 unitary unimodular matrix. Following the SU(2) case write

$$U \equiv \exp\left(\frac{1}{2} i\theta \hat{\mathbf{n}} \cdot \boldsymbol{\lambda}\right)$$

where the λ_i are eight dependent Hermitian traceless 3×3 matrices analogous to the σ_i of SU(2). Canonically these are chosen to be [28]

$$\lambda_1 = \begin{pmatrix} 0 & 1 & \cdot \\ 1 & 0 & \cdot \\ \cdot & \cdot & \cdot \end{pmatrix} \qquad \lambda_2 = \begin{pmatrix} 0 & -i & \cdot \\ i & 0 & \cdot \\ \cdot & \cdot & \cdot \end{pmatrix} \qquad \lambda_3 = \begin{pmatrix} 1 & 0 & \cdot \\ 0 & -1 & \cdot \\ \cdot & \cdot & \cdot \end{pmatrix}$$

$$\lambda_4 = \begin{pmatrix} 0 & \cdot & 1 \\ \cdot & \cdot & \cdot \\ 1 & \cdot & 0 \end{pmatrix} \qquad \lambda_5 = \begin{pmatrix} 0 & \cdot & -i \\ \cdot & \cdot & \cdot \\ i & \cdot & 0 \end{pmatrix} \qquad \lambda_6 = \begin{pmatrix} \cdot & \cdot & \cdot \\ \cdot & 0 & 1 \\ \cdot & 1 & 0 \end{pmatrix}$$

$$\lambda_7 = \begin{pmatrix} \cdot & \cdot & \cdot \\ \cdot & 0 & -i \\ \cdot & i & 0 \end{pmatrix} \qquad \lambda_8 = \frac{1}{\sqrt{3}} \begin{pmatrix} 1 & 0 & 0 \\ 0 & 1 & 0 \\ 0 & 0 & -2 \end{pmatrix} \tag{A.1}$$

where the dots are zeros and we have written them in this fashion to highlight the SU(2) subgroups contained within SU(3). The $\lambda_{1,2}$ have the structure

$$\left(\begin{array}{cc|c} & \sigma_{1,2} & \begin{matrix} 0 \\ 0 \end{matrix} \\ \hline \begin{matrix} 0 & 0 \end{matrix} & & 0 \end{array}\right) \tag{A.2}$$

and hence exhibit the SU(2) isospin subgroup. The $\lambda_{6,7}$ are

$$\begin{pmatrix} 0 & 0 & 0 \\ 0 & & \\ 0 & & \sigma_{1,2} \end{pmatrix} \tag{A.3}$$

and exhibit an SU(2) subgroup called U-spin while the $\lambda_{4,5}$ are related to a third subgroup V-spin. In terms of the basic triplet of Fig. these SU(2) doublets are

$$\text{u,d}(I); \qquad \text{d,s}(U); \qquad \text{u,s}(V)$$

The operator $F_3 \equiv \frac{1}{2}\lambda_3$ is the isospin operator since acting on u, d, s it has eigenvalues $\pm\frac{1}{2}, 0$ respectively. The hypercharge operator is

$$Y = \frac{2}{\sqrt{3}} F_8 \equiv \frac{2}{\sqrt{3}} \cdot \frac{1}{2}\lambda_8 \tag{A.4}$$

Table A.1: *Structure constants of SU(3)*

$f_{123} = 1$
$f_{147} = f_{246} = f_{257} = f_{345} = f_{516} = f_{637} = \frac{1}{2}$
$f_{458} = f_{678} = \frac{\sqrt{3}}{2}$
$d_{118} = d_{228} = d_{338} = -d_{888} = \frac{1}{\sqrt{3}}$
$d_{146} = d_{157} = d_{256} = d_{344} = d_{355} = \frac{1}{2}$
$d_{247} = d_{366} = d_{377} = -\frac{1}{2}$
$d_{448} = d_{558} = d_{668} = d_{778} = -\frac{1}{2\sqrt{3}}$

The commutation relations of the matrices $\frac{1}{2}\lambda_i$ can be obtained by explicit calculation.

$$\left[\frac{1}{2}\lambda_i, \frac{1}{2}\lambda_j\right] = i f_{ijk}\left(\frac{1}{2}\lambda_k\right) \tag{A.5}$$

with the structure constants f_{ijk} having the value in Table A.1 and being antisymmetric under interchange of any pair of indices. The matrices also satisfy anticommutation relations

$$\left\{\frac{1}{2}\lambda_i, \frac{1}{2}\lambda_j\right\} = \frac{1}{3}\delta_{ij} + d_{ijk}\left(\frac{1}{2}\lambda_k\right) \tag{A.6}$$

where the d_{ijk} are symmetric under interchange of indices.

As in the SU(2) case we can generalize these results by defining $F_i \equiv \frac{1}{2}\lambda_i$ satisfying commutation relations

$$[F_i, F_j] = i f_{ijk} F_k \tag{A.7}$$

$(i = 1 \cdots 8)$. A full study of SU(3) then consists of finding $N \times N$ matrices F_i which transform N-dimensional states by

$$\phi \to \phi' = (1 + i\theta\hat{\mathbf{n}} \cdot \boldsymbol{F})\,\phi \tag{A.8}$$

These states form N-dimensional multiplets of SU(3).

A.2 Hadron interaction

Hadrons are defined as particles that interact by the strong interaction. We can subdivide hadrons to baryons and mesons by their spin: baryons are hadrons with half-integer spins (1/2, 3/2, 5/2, ...), and mesons are hadrons with integer spins (0, 1, 2,...). Thus, there are 3 types of the interaction between hadrons, that is, baryon-baryon, meson-baryon and meson-meson interactions.

Baryon-baryon interactions

$$\begin{array}{ll} S=0 & NN \\ S=-1 & \Lambda N-\Sigma N \\ S=-2 & \Xi N-\Lambda\Lambda-\Lambda\Sigma-\Sigma\Sigma \\ S=-3 & \Xi\Lambda-\Xi\Sigma \\ S=-4 & \Xi\Xi \end{array} \tag{A.9}$$

Meson-baryon interactions

$$\begin{array}{ll} S=1 & KN \\ S=0 & \pi N-\eta N-K\Lambda-K\Sigma \\ S=-1 & \pi\Lambda-\pi\Sigma-\bar{K}N-\eta\Lambda-\eta\Sigma-K\Xi \\ S=-2 & \pi\Xi-\eta\Xi-\bar{K}\Lambda-\bar{K}\Xi \\ S=-3 & \bar{K}\Xi \end{array}$$

Meson-meson interactions

$$\begin{array}{ll} S=-2 & K\bar{K} \\ S=-1 & \pi\bar{K}-\eta\bar{K} \\ S=0 & \pi\pi-K\bar{K}-\eta\pi-\eta\eta \\ S=1 & \pi K-\eta K \\ S=2 & KK \end{array}$$

This page is intentionally left blank.

Bibliography

[1] T. Inoue, *et al.*, Prog. Theor. Phys. **124**, 591 (2010).

[2] Y. Ikeda, *et al.*, EPJ Web Conf. **3**, 03007 (2010).

[3] N. Ishii *et al.*, Phys. Rev. Lett. **99**, 022001 (2007).

[4] J. Oller and E. Oset, Nucl. Phys. A **620**, 438 (1997).

[5] J. A. Oller *et al.*, Phys. Rev. D **59**, 074001 (1999).

[6] I. Arisaka, *et al.*, Progress of Theoretical Physics **113**, 1287 (2005).

[7] S. Shinmura, *et al.*, Prog. Theor. Phys. **124**, 125 (2010).

[8] M. I. Haftel and F. Tabakin, Nuclear Physics A **158**, 1 (1970).

[9] M. Taketani *et al.*, Prog. Theor. Phys. **6**, 581 (1951).

[10] D. Lohse, *et al.*, Nucl. Phys. A **516**, 513 (1990).

[11] R. Büttgen, *et al.*, Nuclear Physics A **506**, 586 (1990).

[12] T. Hyodo *et al.*, Phys. Rev. C **85**, 015201 (2012).

[13] S. D. Protopopescu, *et al.*, Phys. Rev. D **7**, 1279 (1973).

[14] R. Kamiński *et al.*, Phys. Rev. D **77**, 054015 (2008).

[15] L. Rosselet, *et al.*, Phys. Rev. D **15**, 574 (1977).

[16] G. Grayer, *et al.*, Nucl. Phys. B **75**, 189 (1974).

[17] C. Froggatt and J. Petersen, Nucl. Phys. B **129**, 89 (1977).

[18] N. M. Cason, *et al.*, Phys. Rev. D **28**, 1586 (1983).

[19] B. Hyams, *et al.*, Nucl. Phys. B **100**, 205 (1975).

[20] J. Gay, *et al.*, Phys. Lett. B **63**, 220 (1976).

[21] A. Martin and E. Ozmutlu, Nucl. Phys. B **158**, 520 (1979).

[22] N. T. H. Xiem and S. Shinmura, Prog. Theor. Exp. Phys. **2014** (2014).

[23] M. J. Matison, *et al.*, Phys. Rev. D **9**, 1872 (1974).

[24] P. Estabrooks, *et al.*, Nucl. Phys. B **133**, 490 (1978).

[25] D. Aston, *et al.*, Nucl. Phys. B **296**, 493 (1988).

[26] R. Mercer, *et al.*, Nucl. Phys. B **32**, 381 (1971).

[27] P. Estabrooks and A. Martin, Nucl. Phys. B **95**, 322 (1975).

[28] M. Gell-Mann, Phys. Rev. **125**, 1067 (1962).

List of Publications by the Author

Journal Publications

1. Ngo Thi Hong Xiem and Shoji Shinmura, "Pion-pion, pion-kaon, and kaon-kaon interactions in the one-meson-exchange model", Progress of Theoretical and Experimental Physics 023D04, doi:10.1093/ptep/ptu001 (2014).

International Conference Publications

1. Ngo Thi Hong Xiem and Shoji Shinmura, "$K^{bar}K^{bar}$ Interaction by vector- and scalar-meson-exchange mechanisms", The 20th International IUPAP Conference on Few-Body Problems in Physics (FB20) Poster session, Fukuoka, Japan (2012).

2. Ngo Thi Hong Xiem and Shoji Shinmura, "The KK Interaction by Meson-Exchange Model", International Workshop on Strangeness Nuclear Physics 2012 (SNP12), Osaka, Japan, Genshikaku Kenkyu, vol. 57, Suppl. 3 (2012).

3. Shoji Shinmura and Ngo Thi Hong Xiem, "K^{bar}-Hyperon Interactions and Possible S-Wave Resonances", Few-Body Systems, vol. 54, issue 7-10, pp 1171-1174 (2013).

4. Ngo Thi Hong Xiem and Shoji Shinmura, "Roles of η channels in $\pi\pi$, $\pi\eta$ and πK scatterings", XV International Conference on Hadron Spectroscopy, Nara, Japan, http://pos.sissa.it/archive/conferences/205/145/Hadron%202013_145.pdf (2013).

5. Ngo Thi Hong Xiem and Shoji Shinmura, "Resonances in meson-meson interaction by one-meson-exchange model", Workshop on J-PARC hadron physics in 2014 Ibaraki Quantum Beam Research Center, Tokai, Ibaraki, Japan (2014).

Domestic Conference Publications

1. Ngo Thi Hong Xiem and Shoji Shinmura "Kaon-Kaon Interaction by Meson-Exchange Mechanisms", The Physical Society of Japan 2012 Fall Meeting, Kyoto (2012).

2. Ngo Thi Hong Xiem and Shoji Shinmura, "On the pipi, Kpi and KK interactions", Workshop on S = -2 and the related Nuclear Physics, Gifu (2012).

3. Ngo Thi Hong Xiem and Shoji Shinmura, "A meson-exchange model of pion-pion, pion-kaon and kaon-kaon interactions", The Physical Society of Japan 2013 (68th) Annual Meeting, Hiroshima (2013).

4. Ngo Thi Hong Xiem and Shoji Shinmura, "A meson-exchange model of pion-pion, pion-kaon and kaon-kaon interactions II", The Physical Society of Japan 2013 Fall Meeting, Kochi (2013).

5. Ngo Thi Hong Xiem and Shoji Shinmura, "σ and κ mesons as broad dynamical resonances in one-meson-exchange model", Nuclear matter in neutron stars investigated by experiments and astronomical observations, Symposium, Atagawa, Shizuoka (2014).

6. Ngo Thi Hong Xiem and Shoji Shinmura, "σ and κ mesons as broad dynamical resonances in one-meson-exchange model", Fourth Joint Meeting of the Nuclear Physics Divisions of the American Physical Society and The Physical Society of Japan, Hawaii (2014).